1-1-2003

Noise analysis of translinear circuits

Lihao Chen
Ryerson University

NOISE ANALYSIS OF TRANSLINEAR CIRCUITS

by

Lihao Chen
(B.Eng., Nanjing, China, June 1994)

A Project

presented to Ryerson University

in partial fulfillment of the

requirement for the degree of

Master of Engineering

in the Program of

Electrical and Computer Engineering

Toronto, Ontario, Canada, 2003

Author's Declaration

I hereby declare that I am the sole author of this project.

I authorize Ryerson University to lend this project to other institutions or individuals for the purpose of scholarly research.

Signature _

I further authorize Ryerson University to reproduce this project by photocopying or by other means, in total or in part, at the request of other institutions or individuals for the purpose of scholarly research.

Signature _

Instructions on Borrower's Page

Ryerson University requires the signatures of all persons using or photocopying this project. Please sign below, and give address and date.

Abstract

Title: Noise Analysis of Translinear Circuits

This project presents noise analysis of translinear circuits, or in general, log-domain filters. Due to the inherit companding behaviour and nonstationary nature of the translinear noise sources, a nonlinear noise analysis method is proposed. Based on the large-signal calculation, the first-order noise and signal-noise intermodulation terms are considered. Overall, two important noise specifications, power spectral density and signal-to-noise ratio, of both static and dynamic translinear circuits are computed. For dynamic translinear circuits, two methods, either combining noise sources and moving them to output, or process them *in situ* and individually, are elaborated. A number of generic examples are illustrated to demonstrate the effectiveness and applications of the methods.

Acknowledgements

Many thanks to my supervisor, Dr. Fei Yuan, for his thoughtful advice, directions, and comments.

Table of Contents

Chapter 1

Introduction

1.1 Translinear Circuit

Due to the ongoing trend towards low-voltage and low-power operation, the area of analog integrated filters is facing serious challenges. As we know, the supply voltage severely restricts the maximum dynamic range achievable using conventional filters. In ultra low-power environments, linear resistors become too large for on-chip integration. The situation is even further complicated by the demand for high operation frequencies and tunable transfer functions.

In order to meet these demands, translinear (TL) circuits were firstly introduced by Barrie Gilbert in 1975. The word "translinear" is coined to state the exponential current-voltage characteristic of bipolar transistors that are central to functioning of these circuits – that is, bipolar transistors' *trans*conductance is *linear* in its collector current [1]. It describes a class of circuits whose large-signal behavior hinges on the extraordinarily precise exponential current-voltage characteristic of bipolar transistors and the intimate thermal contact and close matching of monolithically integrated devices.

Gilbert also meant the word to convey the notion of analysis and design techniques (e.g., the TransLinear Principle (TLP)) that bridge the gap between the well-established domain of linear-circuit design and the largely uncharted domain of nonlinear-circuit design, for which precious little can be said in general [2]. In effect, we can characterize the TLP as a translation through the exponential current–voltage relationship of a linear constraint on the voltages in a circuit (i.e., Kirchhoff's voltage law) into a product-of-power-law constraint on collector currents flowing in the circuit.

In 1980s, Evert Seevinck made significant contributions to the state of the art of translinear-circuit design by developing systematic techniques for the analysis and synthesis of these circuits [3,4]. Since the mid-1990s, there has been an explosion of interest in translinear circuits, primarily because of the development of the class of dynamic translinear circuits, which had its origins in 1979 in the work of Robert Adams [5]. Although he does not appear to have made a connection between his own ideas and

the growing body of work on translinear circuits, Adams proposed a method of implementing large-signal–linear, continuous-time filters using linear capacitors, constant current sources, and translinear devices, which he called *log-domain filtering*, because all of the filtering occurred on log-compressed voltage state variables using translinear devices. The concept of log-domain filtering remained in obscurity for over a decade, only to be independently rediscovered by Seevinck. In 1990, Seevinck presented a first-order filter, which he dubbed a *companding current-mode integrator* [6]. Unfortunately, it appears that neither Seevinck nor Adams had a clear idea of how to generalize their ideas to implement filters of higher order. In 1993, encouraged by Adams to pursue the idea of log-domain filtering, Doug Frey introduced a general method for synthesizing log-domain filters of arbitrary order using a state-space approach and he presented a highly modular technique for implementing such filters [7].

Jan Mulder and his colleagues coined the phrase *dynamic translinear circuits* and have made the clearest connection between translinear circuits and log-domain filters [8-12]. They have extended Seevinck's translinear analysis and synthesis methodology to encompass dynamic constraints based on what they have called the dynamic translinear principle, with which we can express capacitive currents embedded within translinear loops directly in terms of products of the currents flowing through translinear devices and their time derivatives. Dynamic translinear circuit techniques have been successfully applied to the structured design of both linear dynamical systems (e.g., log-domain filters) and nonlinear dynamical systems (e.g., RMS-DC converters, oscillators, phase detectors, and phase-locked loops).

1.2 Electrical Noise

Electrical noise, one of the most important topics in circuit analysis and design, will be discussed in this paper. The noise phenomena considered here are caused by the small current and voltage fluctuations that are generated within the devices themselves, and we specifically exclude extraneous pickup of man-made signals that can also be a problem in high-gain circuits.

The study of noise is important because it represents a lower limit to the size of electrical signal that can be amplified by a circuit without significant deterioration in signal quality. Noise also results in an upper limit to the useful gain of an ampifier, because if the gain is increased without limit, the output stage of the circuit will eventually begin to limit (that

is, cut off or saturate) on the amplified noise from the input stages.

Furthermore, static translinear (STL) circuits do not have a perticularly good reputation in terms of noise, and it is likely that dynamic translinear (DTL) circuits inherit those noise characteristics. Therefore, it is very important to analyze this important non-ideal aspect.

Power Spectral Density (PSD) and Signal-to-Noise-Ratio (SNR) are two primary specifications describing the noise beharivour of analog circuits. Since translinear circuits are explicitly based on the exponential behaviour of bipolar transistors, they are inherently non-linear, even when they exhibit an externally-linear transfer characteristic. As a result, intermodulation between signals and noise is generated. The situation is further complicated by the fact that the internal noise sources are non-stationary. The transistor currents in a TL circuit are signal-dependent. For example, the transistor shot noise sources are modulated by the signals being processed.

A number of noise analysis methods for STL and DTL circuits have been proposed previously. However, most of these approaches are quasi-linear and quasi-stationary, these methods cannot adequately account for the non-linear and non-stationary properties of noise in TL circuits. It is also important to note that most circuit simulators do not facilitate non-linear noise analysis.

In the area of non-linear signal processing theory, a lot of efforts have been made on noise analysis. These results can be adopted to the noise analysis in TL circuits.

1.3 Outline of the Project

The basic noise characteristics are stated in Chapter 2. Three major noise sources: shot, thermal and $1/f$ noise sources are discussed, as well as their influence in active components of circuits. Then, the noise behaviour is analyzed in terms of system representation.

Chapter 3 discusses the basic principle of TL circuits. Two models, a first-order model and a high-order model are given, from the system perspective. On the other hand, from the circuit analysis point of view, both static and dynamic TL circuits are discussed. All the analyses are based on ideal transistor behaviour, i.e., ignoring noise influence.

Chapter 4 is devoted to explore methods in analyzing noise characteristics in TL circuits, several important definitions are clarified. By comparing the noise sources, we are able to focus on the ones that have greatest influence on circuit performance. Finally, serveral typical STL and DTL circuits are analyzed.

Chapter 5 proposes an alternative noise analysis method for DTL filters. Unlike what is proposed in chapter 4, all noise sources are processed *in situ* and individually. This is based on the assumption that all noise sources are independent to each other.

Finally, Chapter 6 concludes the project.

Chapter 2

Noise Characterization in Electronic Circuits

2.1 Shot Noise

Shot noise is always associated with a direct-current flow and is present in diodes and bipolar transistors [20,21].

The origin of shot noise can be explained by considering a diode. The forward current of the diode I is composed of holes from the p region and electrons from the n region, which have sufficient energy to overcome the potential barrier at the junction. Once the carriers have crossed the junction, they diffuse away as minority carriers.

The passage of each carrier across the junction is a purely random event and is dependent of the carrier having sufficient energy and a velocity directed toward the junction. Thus an external current I, which appears to be a steady current, is in fact, composed of a large number of random independent current pulses, as shown in Figure 2.1, where $I_D = 1$, is the average current.

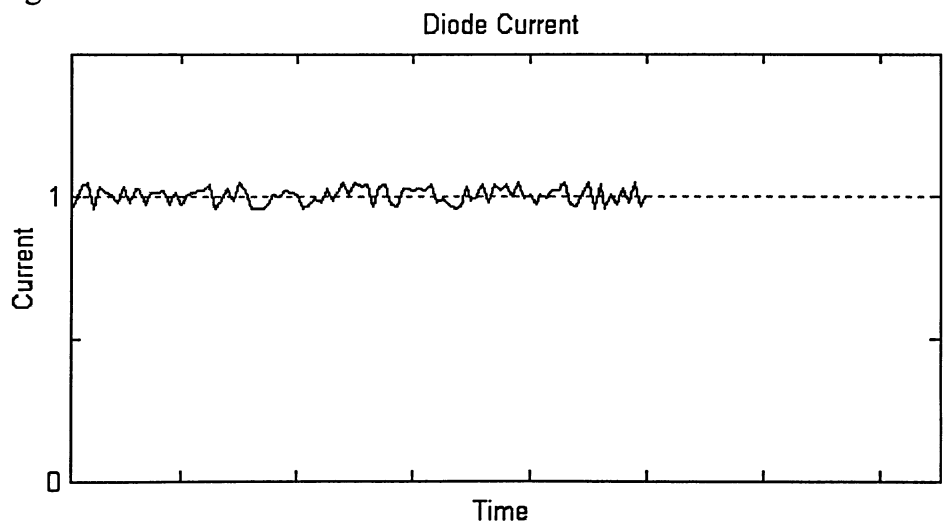

Figure 2.1 Diode current I as a function of time.

The fluctuation in I is termed *shot noise* and is generally specified in terms of its mean-square variation about the average value. This is written as $\overline{i^2}$, where

$$\overline{i^2} = \overline{(I - I_D)^2} = \lim_{T \to \infty} \frac{1}{T} \int_0^T (I - I_D)^2 \, dt \qquad (2.1.1)$$

Since the current I is composed of a series of random independent pulses with average value I_D, then the resulting noise has a mean-square value

$$\overline{i^2} = 2qI_D\Delta f \qquad (2.1.2)$$

where $q = 1.602 \times 10^{-19}$ C, the charge of an electron,

Δf = Bandwidth in Hertz,

I_D = Direct current.

From equation (2.1.2), we can see the noise current has a mean-square value that is directly proportional to the bandwidth Δf. Thus, the noise-current spectral density $i^2/\Delta f$ (A^2/Hz) is independent of frequency. Noise with such a characteristic is called *white noise*. It is valid until the frequency becomes comparable to $1/\tau$, where τ is the carrier transit time through the depletion region. For most practical electronic devices, τ is extremely small and (2.1.2) is accurate well into gigahertz region [20].

The effect of shot noise can be represented in the low-frequency, small-signal equivalent circuit of the diode by inclusion of a current generator shunting the diode, as shown in Figure 2.2.

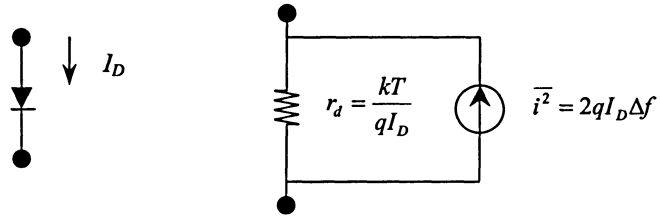

Figure 2.2 Junction diode small-signal equivalent circuit with noise

Note: In Figure 2.2, the arrow in the current source is only to identify the generator as a current source, not indicating its polarity, because this noise signal has a random phase and is defined solely in terms of its mean-square value.

Because the amplitude distribution of shot noise is Gaussian. From the definition of Gaussian PDF (probability density function), we get the variance σ^2 and the standard deviation σ as follows:

$$\sigma^2 = \overline{(I - I_D)^2} = \overline{i^2}, \qquad \sigma = \sqrt{2qI_D\Delta f}. \qquad (2.1.3)$$

2.2 Thermal Noise

Unlike shot noise, thermal noise is generated by a completely different mechanism. In conventional resistors, it is due to the thermal motion of electrons and is unaffected by the presence or absence of a direct current [20,21]. Therefore, we expect that it is related to absolute temperature T.

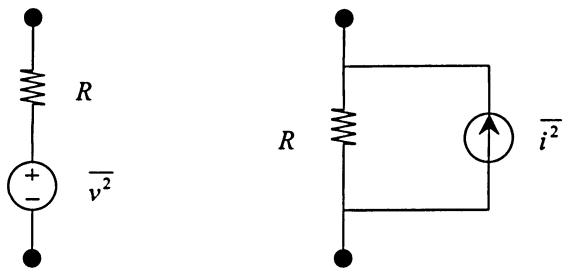

(*a*) (*b*)

Figure 2.3 Resistor model including thermal noise source through
(*a*). a series voltage generator
(*b*). a shunt current generator

In a resistor R, thermal noise can be represented by a series voltage generator $\overline{v^2}$, or by a shunt current generator $\overline{i^2}$ as in Figure 2.3.

These representations are equivalent:

$$\overline{v^2} = 4kTR\Delta f, \qquad \overline{i^2} = 4kT\frac{1}{R}\Delta f, \tag{2.2.1}$$

where $k \approx 1.38 \times 10^{-23}$ J/K (Joules/Kelvin), Boltzmann's constant and
$4kT = 1.66 \times 10^{-20}$ V-C at room termperature (300°K).

Equations in (2.2.1) show that the noise spectral density of thermal noise is independent of frequency. Thermal noise is white in nature.

For example, a 1 KΩ resistor exhibits the termal noise spectral density at room temperature: $\overline{v^2}/\Delta f = 16\times10^{-18}(\mathrm{V^2/Hz})$, or $\overline{i^2}/\Delta f = 1.6\times10^{-23}(\mathrm{A^2/Hz})$. It is equivalent to the shot noise of a 50μA direct current: $\overline{i^2}/\Delta f = 2qI_D = 1.6\times10^{-23}(\mathrm{A^2/Hz})$.

The amplitude distribution of thermal noise is Gaussian. Since both shot and thermal

noise have a flat frequency spectrum and a Gaussian amplitude distribution, they are indistinguishable once they are introduced to a circuit.

2.3 Flicker Noise

This type of noise is found in all active devices, as well as some discrete passive elements such as carbon resistors. The origins of flicker noise are varied, but in bipolar transistors it is caused mainly by traps associated with contamination and crystal defects in the emitter-based depletion layer [20,21]. These traps capture and release carriers in a random fashion. It is always associated with the flow of a direct current and displays a spectral density of the form

$$\overline{i^2} = K\frac{I^a}{f^b}\Delta f\,, \tag{2.3.1}$$

where

Δf = small bandwidth at frequency f,
I = direct current in amps,
K = a constant for a particular device,
a = is a constant in the range 0.5 to 2, and
b = a constant of about unity.

In most cases, a=b=1. Thus, equation (2.3.1) becomes

$$\overline{i^2} = K\frac{I}{f}\Delta f\,. \tag{2.3.2}$$

The noise spectral density thus has a $1/f$ frequency characteristic. Hence, it is also called $1/f$ noise.

We notice that the mean-square value of a flicker noise signal as given by (2.3.2) contains an unknown constant K. This constant not only varies by orders of magnitude from one device type to the next, but it can also vary widely for different transistors or integrated circuits from the same process wafer that has undergone identical fabrication steps. This is due to contamination and crystal imperfections, which are factors that can vary randomly even on the same silicon slice.

However, experiments have shown that if a typical value of K is determined from measurements on a number of devices from a given process, then this value can be used

to predict average or typical flicker noise performance for integrated circuits from that process. From measurements, the amplitude distribution of flicker noise is often non-Gaussian.

2.4 Noise Equivalent Circuits

In this section, we will consider the small-signal equivalent circuit of typical IC (integrated circuit) devices.

2.4.1 Junction Diodes

The equivalent circuit of a junction diode is shown in Figure 2.4 [20]. r_s is a physical resistor due to the resistivity of the silicon, it exhibits thermal noise. Shot noise and flicker noise are combined to be represented as a current generator in shunt with r_d.

Equation (2.4.1) gives the noise generator:

$$\begin{aligned} \overline{v_s^2} &= 4kTr_s\Delta f, \\ \overline{i^2} &= 2qI_D\Delta f + K\frac{I_D}{f}\Delta f. \end{aligned} \tag{2.4.1}$$

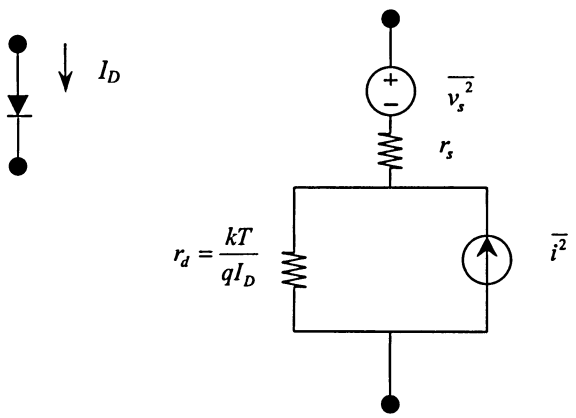

Figure 2.4 Complete diode small-signal equivalent circuit with noise

2.4.2 Bipolar Transistors

In bipolar transistors, from the base region, carriers entering the collector-base depletion region are accelerated by the field existing there and swept across this region to the collector. This procedure is purely random, so I_C and I_B show full shot noise.

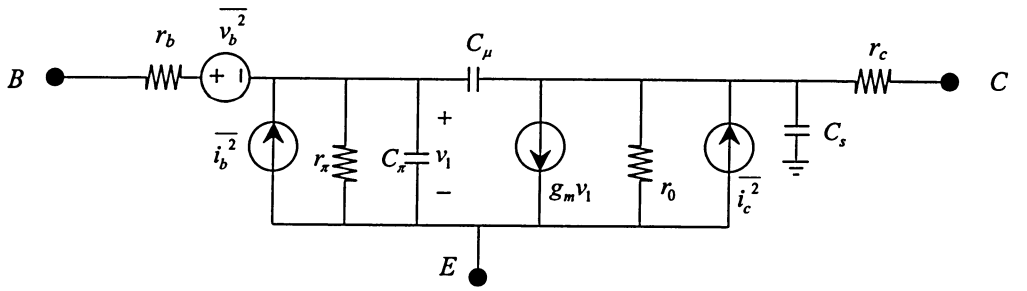

Figure 2.5 Complete bipolar transistor small-signal equivalent circuit with noise sources

Transistor base resistors r_b and r_c are physical resistors and thus have thermal noise. Comparing with the high-impedance collector node, r_c is usually negligible. The resistors r_π and r_0 are fictitious resistors that are used for modeling purpose only, they do not exhibit thermal noise.

Since all the noise sources are separate, independent physical mechanisms, the mean-square values are:

$$\begin{aligned} \overline{v_b^2} &= 4kTr_b\Delta f, \\ \overline{i_c^2} &= 2qI_C\Delta f, \\ \overline{i_b^2} &= 2qI_B\Delta f + K\frac{I_B}{f}\Delta f. \end{aligned} \tag{2.4.2}$$

In analog circuit design and analysis, we usually use a simplified equivalent circuit to illustrate noise influence of bipolar transistors [18], as shown in Figure 2.6.

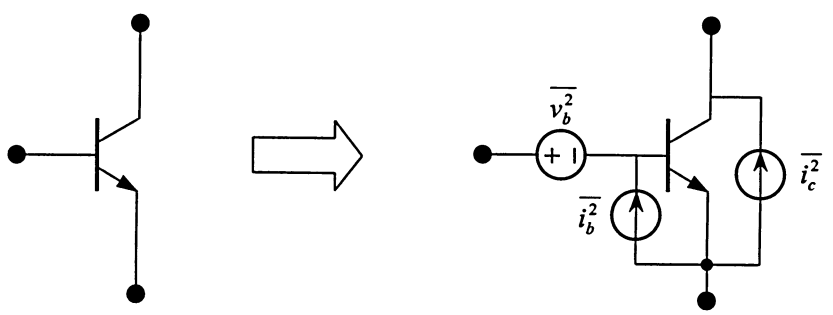

Figure 2.6 A simplified equivalent circuit of BJTs with noise sources

2.4.3 Field-Effect Transistors

In FET, the resistive channel joining source and drain is modulated by the gate-source voltage so that the drain current is controlled by the gate-source voltage. Since the channel material is resistive, it exhibits thermal noise. Flicker noise also exists and can be represented by a drain-source current generator[21]. These two sources can be lumped into one noise generator $\overline{i_d^2}$.

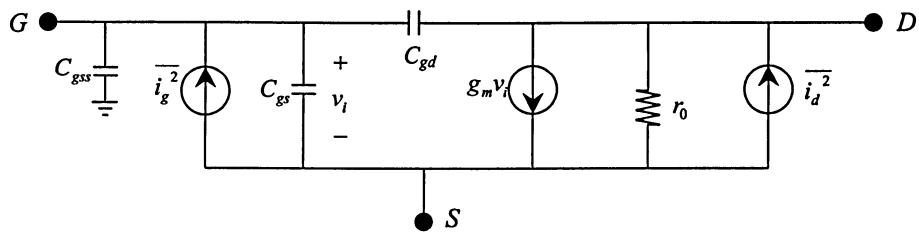

Figure 2.7 Complete FET small-signal equivalent circuit with noise sources

$$\overline{i_g^2} = 2qI_G\Delta f,$$
$$\overline{i^2} = 4kT\left(\frac{2}{3}g_m\right)\Delta f + K\frac{I_D}{f}\Delta f, \qquad (2.4.3)$$

where I_G = gate leakage current,

I_D = drain bias current,

K = a constant for a given device, and

g_m = the device transconductance at the operating point.

2.4.4 Resistors

Monolithic and thin-film resistors show thermal noise [21]. Please refer to equation (2.2.1) for its generator parameters. Figure 2.4 illustrates its circuit representation.

As mentioned in Section 2.3, discrete carbon resistors also exhibit flicker noise, and this should be considered if such resistors are used as external components of integrated circuits [20].

2.5 Stochastical Representation of Noise Signals

Intuitively, noise is often visualised as an undesirable, fuzzy waveform corrupting a signal, as illustrated in Figure 2.1. Therefore, the noise waveform can not be represented exactly. Instead, the theory of stochastic processes or random processes is used to find its average spread.

Let $x(t)$ be a random variable in the time-domain. Like any random variable, $x(t)$ has a mean $\mu_x(t)$ and variance $\sigma_x^2(t)$. While it is meaningless to ask what the value of $x(t)$ is at a given time t (for $x(t)$ represents a collection of waveforms, which are not individually known), the mean and variance provide useful imformation about the averages of the ensemble.

In communication systems, we are often interested in frequency-domain representation, *i.e.*, Fourier transforms of time-domain waveforms [19]. It may be asked what the Fourier transform of a stochastic process $x(t)$ is. In principle, one may consider the Fourier transform of each member of the ensemble $x(t)$ (or its square for the power), to obtain a new ensemble $X(f)$, parameterized by the frequency f. Such definition is not, however, strictly correct, simply because members of the $x(t)$ ensemble may not have finite energy and hence cannot be Fourier-transformed. Nevertheless, a technically correct definition that retains this intuition is possible. The transformed ensemble $X(f)$ is a stochastic process in frequency, with mean $\mu_X(f)$ and variance $\sigma_X^2(f)$ providing information about its averages. Actually, the autocorrelation function of $x(t)$ is a much useful concept in noise analysis, both from the time-domain and frequency-domain points of view [19].

The autocorrelation function $R_{xx}(t,\tau)$ is the expected value of $x(t)x(t+\tau)$. The function denotes the correlation between values of the stochastic process at different times. If $R_{xx}(t,\tau)$ depends only on τ, *i.e.*, only on the time difference between the two timepoints, $x(t)$ is called a *stationary stochastic process*; if there is a dependence on t as well, it is called *nonstationary*.

2.5.1 Stationary Noise

If $x(t)$ is stationary, the Fourier transform of its autocorrelation $R_{xx}(\tau)$ is called the power spectral density of $x(t)$, and denoted by $S_{xx}(f)$. The power spectral density (PSD) is a useful characterization of a stochastic process, for it can be measured directly on a

sprectrum analyzer. This is because there is a direct connection between PSD and the Fourier transforms of the squares of the stochastic process ensemble denoted by $X(f)$ above.

It can be shown that the mean value of the Fourier transforms of the squared process, at a given value of frequency f, is equal to $S_{xx}(f)$. Further, two random variables $X(f_1)$ and $X(f_2)$ can be shown to be uncorrelated if $f_1 \neq f_2$. Therefore, spectrum analyzers display Fourier transforms of the squared input, averaged over separated sections of time, thus approximating an ensemble average and measuring PSD directly. Another property of PSD is that its integral over frequency equals the variance of $x(t)$. This is the total noise power, an important figure of merit.

If PSD is independent of frequency, *i.e.*, $S_{xx}(f)$ is a constant, the process is known as white noise. This corresponds to the autocorrelation function $R_{xx}(\tau)$ being a Dirac function in τ, implying that neighbouring points of the process are totally uncorrelated. Many noise sources in circuits can be modeled adequately as white noise, such as thermal noise of resistors and shot noise of semiconductors [20,21].

The concepts of stationary suffice for noise analysis in systems in a small linear region at the DC operating point, such as linear amplifiers. However, some components in RF systems, such as mixers, do not operate in a small region around a quiescent point, but have large-signal swings that are crucial to their operation. Stationary concepts no longer suffice for describing noise in such systems. For example, consider a switch that turns on and off periodically, either passing its input through or blocking it completely. This ideal switch mixer cannot be time-invariant, since the periodic switch control makes the output dependent on the time in the cycle that an input is applied. Furthermore, if the input is a stationary stochastic process, the output is no longer stationary, for its power is zero when the switch is off, whereas it is the same as that of the input when the switch is on. Since the output power varies with time, the output noise is not stationary.

2.5.2 Non-stationary Noise

If $x(t)$ is nonstationary, its autocorrelation function $R_{xx}(t,\tau)$ is a function of t. When the dependence on t is periodic or quasiperiodic, the process is called cyclostationary [22]. Cyclostationary processes usually arise in systems such as mixers.

The autocorrelation function of a cyclostationary process can be expanded in a Fourier series in t:

$$R_{xx}(t,\tau) = \sum_k R_k(\tau) e^{jk2\pi f_0 t}, \qquad (2.5.1)$$

where $R_k(\tau)$ = harmonic autocorrelation function.

Typically, a finite number of harmonics are sufficient to dscribe the process. The Fourier transform of $R_k(\tau)$, denoted by $S_k(f)$, is called the harmonic power spectral density (HPSD).

If $x(t)$ is cyclostationary, it can further be shown that the Fourier transformed process $X(f)$ is no longer uncorrelated at different values of f. In fact, $X(f)$ and $X(f+if)$ can be shown to be correlated with value $S_k(f)$. This phenomenon is known as frequency correlation.

The stationary part of the power spectrum (*i.e.*, the component that is independent of t) is given by $S_0(f)$ and denotes the average noise power. This is actually the only output quantity of interest, see chapter 4 for more details. However, it is very important to keep track of the other HPSDs during noise analysis of time-varying system, for they can affect $S_0(f)$ at the outputs.

2.6 System Representation for Noise Analysis

Electronic circuits as dynamical systems are modeled with partial and ordinary differential equations, transfer functions, finite-state machines, etc. For noise analysis, a system of differential/algebraic equations and transfer functions are most appropriate. Transfer functions are especially useful, because they represent the system components in frequency domain, the domain of choice for RF design, and as the basis for input-output black-box and reduced-order models [19].

Let us define a system as mapping an input $x(t)$ into an output $y(t)$, through $y = H(x)$. A system H is said to be:

a). linear: $H(ax_1 + bx_2) = aH(x_1) + bH(x_2)$,

b). time-invariant: $Y(t) = H(x(t)) \Rightarrow Y(t+\tau) = H(x(t+\tau))$.

For a linear system, the impulse response is given by,

$$h(t,u) = H(\delta(t-u)).$$

For an arbitrary input, the system output is given by,

$$H(x)(t) = \int_{-\infty}^{\infty} x(u)h(t,u)du\,. \qquad (2.6.1)$$

If the system is time-invariant, then $h(t,u) = h(t-u)$. If the input to an LTI system is a complex exponential at frequency f, $x(t) = \exp(j2\pi ft)$, then the output is

$$H(x)(t) = H(f)\exp(j2\pi ft), \qquad (2.6.2)$$

where $H(f)$ is the Fourier transform of the impulse response $h(t)$,

$$H(f) = \int_{-\infty}^{\infty} h(t-u)\exp(-j2\pi f(t-u))du, \qquad (2.6.3)$$

and is called the system transfer function. For an arbitrary input with Fourier transform $X(f) = F\{x(t)\}$, the output is

$$H(x)(t) = \int_{-\infty}^{\infty} H(f)X(f)\exp(j2\pi ft)df\,, \qquad (2.6.4)$$

with the Fourier transform

$$Y(f) = F\{H(x)(t)\} = H(f)X(f)\,. \qquad (2.6.5)$$

By analogy with (2.6.3), the system transfer function $H(t,f)$ for a linear time-varying (LTV) system is defined by

$$H(t,f) = \int_{-\infty}^{\infty} h(t,u)\exp(-j2\pi f(t-u))du\,. \qquad (2.6.6)$$

Note that, in contrast to $H(f)$ in (2.6.3), $H(t,f)$ in (2.6.6) is a function of both f and t. If the input to an LTV system H is $x(t) = \exp(j2\pi ft)$, then the output is

$$H(x)(t) = H(t,f)\exp(j2\pi ft), \qquad (2.6.7)$$

which is a generalization of (2.6.2) to LTV systems. For an arbitrary input with $X(f) = F\{x(t)\}$, the output is

$$H(x)(t) = \int_{-\infty}^{\infty} H(t,f)X(f)\exp(j2\pi ft)df\,. \qquad (2.6.8)$$

A linear system is (linear) periodically time-varying (LPTV), if the impulse response is periodic in t:

$$H(t+\tau,t) = H(t+T+\tau,t+T), \qquad (2.6.9)$$

with Fourier series respresentations for the impulse response and the transfer function

$$H(t+\tau,t) = \sum_{n=-\infty}^{\infty} h_n(\tau)\exp(j2\pi nf_c t), \qquad (2.6.10)$$

$$H(t,f) = \sum_{n=-\infty}^{\infty} H_n(f+nf_c)\exp(j2\pi nf_c t), \qquad (2.6.11)$$

where $H_n(f) = F\{h_n(\tau)\}$, the harmonic transfer functions, and

f_c = fundamental frequency.

If the input to an LPTV system H is $x(t) = \exp(j2\pi ft)$, then the output is

$$H(x)(t) = \sum_{n=-\infty}^{\infty} H_n(f + nf_c)\exp(j2\pi n(f + nf_c)t), \tag{2.6.12}$$

with the Fourier transform

$$Y(f) = \sum_{n=-\infty}^{\infty} H_n(f)X(f + nf_c), \tag{2.6.13}$$

where $X(f)$ is the Fourier transform of the input. This is the generalization of (2.6.5) to LPTV systems.

If a single complex exponential at frequency f is input to an LTI system, the output is also a single complex exponential at frequency f, with an amplitude set up by the transfer function $H(f)$. Then, for a LPTV system, the output is a summation of complex exponentials at freqencies $f + nf_c$, where f_c is the fundamental frequency. Finally, for a nonlinear periodically time-varying system, the output signal is a summation of complex exponentials at frequencys $kf + nf_c$, where $k = 1, \cdots, \infty$, $n = -\infty, \cdots, \infty$ [19].

Chapter 3

Translinear Circuit Analysis

An important branch of analog circuits is the *translinear* group. Translinear circuits exploit the precise proportionality of transconductance to collector current in bipolar junction transistors so as to result in fundamentally exact, temperature-insensitive behavior [1]. This relationship, however, need not appear explicitly in the analysis of translinear circuits.

Translinear circuits operate entirely in the current domain, and the algebraic functions they generate may have many forms, incorporating products, quotients, power terms with fixed exponents, which may be integral or non-integral, positive or negative, and sums and differences. The main distinguishing feature of a translinear circuit is that it uses an even number of forward-biased PN junctions that are arranged in one or more loops, with as many junctions connected in one polarity direction as in the other.

> A translinear circuit is one having all inputs and outputs in the form of currents and whose primary function arises from the exploitation of the logarithmic behavior of forward-biased PN junctions, which are arranged in pairs so as to result in fundamentally exact, temperature-independent transformations in the amplitude domain [2].

Due to the continuing trend towards lower supply voltages and low-power operation, the interest in the application of *companding* techniques is increasing. The word *companding* is coined from *comp*ressing and ex*panding* [6]. And the realisation of companding signal processors is translinear filters.

In Section 3.1, an abstract approach is pursued to describe the general principle of distortionless companding. At a less abstract level, Section 3.2 is geared toward the inherent companding characteristics of translinear circuits.

3.1 A General Approach to Companding

The companding technique, a combination of compressing and expanding, gets more and more interest since continuing trend towards lower supply voltages. The traditional set up is shown in Figure 3.1(a).

The input signal is first compressed, in block *C*, before it is applied to *H*, where the actual signal processing is performed. At the output of *H*, the signal is restored through an expansion in block *E*. The benefit of companding is that a signal with a certain dynamic range (DR) can be processed in a system block with a smaller DR than the signal, illustated in Figure 3.1(b).

The DR of the signal processing block *H* is limited on two sides. The upper level stands for the maximum amplitude of the input signal without generating distortion, while the lower level indicates the smallest signal that can be processed. Therefore, the influence of companding also has two sides. At the upper level, large input signals are attenuated by the compressor *C* down to a level where *H* can handle without causing excessive distortion. At the lower level, small input signals are amplified by *C* to a level well above the noise floor of *H*, making the signal less susceptible to noise and interference.

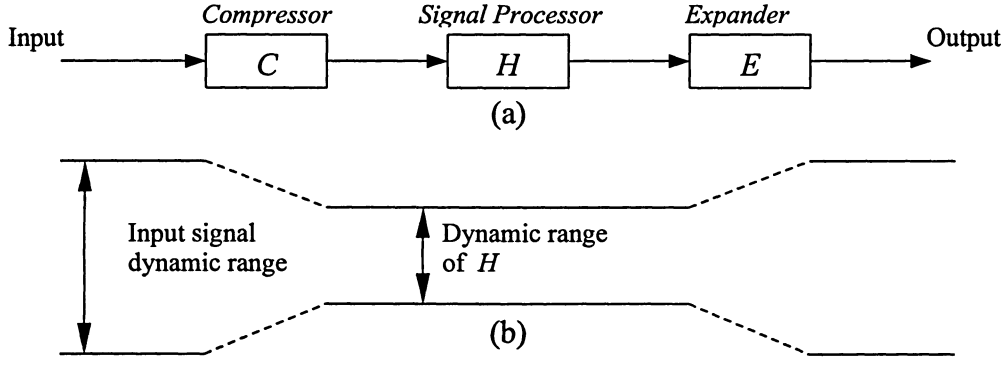

Figure 3.1 (a) Traditional companding system.
(b) The dynamic range of the signal along the path

In practice, the bandwidth of *H* is limited, resulting in a frequency-dependent transfer function. It can be either intentional to filter the input signal, or unwanted caused by parasitic reactive elements. Anyway, the distortion arises.

3.1.1 Syllabic and Instantaneous Companding

Companding system can be divided into two major classes: syllabic and instantaneous,

with respect to the difference in transfer functions of compressor and expander.

In a syllabic comanding system, the transfer function of C is a function of some measures of the average strenght of the signal [32].

In an instantaneous companding system, the output of C is a function of the instantaneous value of the input signal [24, 28]. In other words, the transfer function is static and non-linear.

3.1.2 A First-Order Model

To describe a distortionless companding system, a dynamic transfer function is required. Here, we use a single linear integrator to model the first-order dynamic system. In principle, other first-order dynamic transfer functions, such as a differentiator, can also be used here. The choice of an integrator complies with the general application of the integrator as the basic building block for filters [13].

It is sufficient to model only the expansion function E, since the compression function can be derived from E [11]. The basic model is shown in Figure 3.2. All signals are implicitly a function of time t.

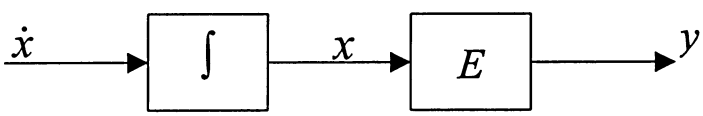

Figure 3.2 The two basic functions of a companding integrator

In an instantanous companding system, the output signal y is a function of the instantaneous value of the integrator output x.

$$y(t) = E(x(t)). \tag{3.1.1}$$

For example, in a log-domain filter, $y(t) = e^{x(t)}$.

In a syllabic companding system, the expansion function is controlled by one or more time-variant signals $g_i(x(t), t)$, where $i \in [1,\ldots,N]$, which can be represented by a column vector $\vec{g}(x(t),t)$.

In general, the transfer function E includes both instantaneous and syllabic companding:

$$y(t) = E(x(t), \vec{g}(x(t),t)). \tag{3.1.2}$$

In addition, E is a strictly monotonous function with respect to x. So, E has an inverse

function E^{-1}, and x can be obtained by:

$$x(t) = E^{-1}(y(t), \vec{g}(x(t), t)). \tag{3.1.3}$$

However, the signal $\dot{x}$ has to be supplied. The question is what this signal should be in order to obtain a system with a linear transfer function from $\dot{y}$ to y, the input and output signal, respectively, of the complete companding integrator.

From equation 3.1.2, we can get an expression of $\dot{y}$:

$$\dot{y} = \frac{\partial E}{\partial x}\dot{x} + \nabla_g E \cdot (\frac{\partial \vec{g}}{\partial x}\dot{x} + \dot{\vec{g}}). \tag{3.1.4}$$

where $\nabla_g E = \left(\frac{\partial E}{\partial g_1}, \cdots, \frac{\partial E}{\partial g_N}\right)$.

From equation 3.1.4, the signal $\dot{x}$ can be found:

$$\dot{x} = \frac{\dot{y} - \nabla_g E \cdot \dot{\vec{g}}}{\frac{\partial E}{\partial x} + \nabla_g E \cdot \frac{\partial \vec{g}}{\partial x}}. \tag{3.1.5}$$

3.1.3 An *n*th-Order Model

In general, the dynamic transfer function of a companding system is of order n. So, the inputs and outputs of these internal integrators are $\dot{x}_j$ and x_j, where $j \in [1,\ldots,n]$, through n different expansion functions E_j, then resulting in n output signals y_j, represented by vectors $\dot{\vec{x}}$, $\vec{x}$, $\vec{E}$ and $\vec{y}$, respectively [12]. So, the output signal vector can be described by:

$$\vec{y}(t) = \vec{E}(\vec{x}(t), \vec{g}(\vec{x}(t), t)). \tag{3.1.6}$$

So, the first-order time derivative is:

$$\dot{\vec{y}} = \mathbf{E}_x \dot{\vec{x}} + \mathbf{E}_g(\mathbf{G}_x \dot{\vec{x}} + \dot{\vec{g}}), \tag{3.1.7}$$

where $\mathbf{E}_x$, $\mathbf{E}_y$, and $\mathbf{G}_x$ are Jacobian matrices given by:

$$\mathbf{E}_x = \begin{bmatrix} \frac{\partial E_1}{\partial x_1} & \cdots & \frac{\partial E_1}{\partial x_n} \\ \vdots & & \vdots \\ \frac{\partial E_n}{\partial x_1} & \cdots & \frac{\partial E_n}{\partial x_n} \end{bmatrix}, \mathbf{E}_g = \begin{bmatrix} \frac{\partial E_1}{\partial g_1} & \cdots & \frac{\partial E_1}{\partial g_N} \\ \vdots & & \vdots \\ \frac{\partial E_n}{\partial g_1} & \cdots & \frac{\partial E_n}{\partial g_N} \end{bmatrix}, \mathbf{G}_x = \begin{bmatrix} \frac{\partial g_1}{\partial x_1} & \cdots & \frac{\partial g_1}{\partial x_n} \\ \vdots & & \vdots \\ \frac{\partial g_N}{\partial x_1} & \cdots & \frac{\partial g_N}{\partial x_n} \end{bmatrix}.$$

So, the input vector $\dot{\vec{x}}$ is:

$$\dot{\vec{x}} = (\mathbf{E}_x + \mathbf{E}_g \mathbf{G}_x)^{-1}(\dot{\vec{y}} - \mathbf{E}_g \dot{\vec{g}}). \tag{3.1.8}$$

The system is linear in the n derivatives $\dot{x}_j$, where "$(\cdot)^{-1}$" denotes the inverse matrix operation.

3.2 Key Idea – Translinear Principles

Both static translinear (STL) and dynamic translinear (DTL) circuits exploit the exponential large-signal transfer function of the bipolar transistor or the MOS transistor in the weak inversion region.

The collector current of a bipolar transistor in the active region is given by [20]:

$$I_C = A \cdot J_S(T) \cdot e^{\frac{V_{BE}}{mU_T}}, \tag{3.2.1}$$

where I_C is the collector current,

V_{BE} is the base-emitter voltage,

A = area of the junction,

$J_S(T)$ = junction reverse saturation current density,

m = ideality factor (typically in the range of from 1 to 2),

U_T is the thermal voltage $kT/q \approx 26$ mV, at room temperature 300 °K,

k is the Boltzmann's constant, $\approx 1.38 \times 10^{-23}$ J/K,

T is the temperature in degrees Kelven (°K), and

q is the charge of an electron, $\approx 1.602 \times 10^{-19}$ C.

If we take the partial derivative of I_C over V_{BE}, it comes with:

$$g_m = \frac{\partial I_C}{\partial V_{BE}} = \frac{\partial (A \cdot J_S(T) \cdot e^{\frac{V_{BE}}{mU_T}})}{\partial V_{BE}} = \frac{A \cdot J_S(T) \cdot e^{\frac{V_{BE}}{mU_T}}}{mU_T} = \frac{I_C}{mU_T}. \tag{3.2.2}$$

As we can easily see, from equation (3.2.2), that the small-signal transconductance g_m of a bipolar transistor is linear to its collector current I_C, and is dependable over six to eight decades [2].

3.2.1 Static Translinear Principle

From equation (3.2.1), the base-emitter voltage exhibits a logarithmic relationship to the junction current:

$$V_{BE} = mU_T \ln\left(\frac{I_C}{A \cdot J_S(T)}\right). \tag{3.2.3}$$

Here, $J_S(T)$ is assumed to scale precisely with junction area; although this is not entirely accurate, in general, due to edge effects, it is safe to make this assumption [2]. Throughout this analysis, it will be assumed that all transistors in a given circuit are

operating at the same temperature.

Equation (3.2.1) (and, thus, Equation (3.2.3)) is an idealization. In practice, many effects conspire to damage this much-to-be-desired ideal, including various carrier-transport related effects at high- and low-current-density (which cause the factor m to be current dependent) and resistance components beyond the intrinsic device. These second order effects may often represent a major limitation to accuracy. The designer of translinear circuits soon becomes aware of this and can, for example, utilize symmetrical configurations that exhibit cancellation of error terms or design special transistor geometries to fit the requirements.

In practice, the logarithmic relationship holds very well over six decades of collector current, from about 100-pA to 100-μA for a typical, small-geometry, 25-micron diameter emitter, and is still useful for collector currents up to around 1-mA [2].

The STL principle applies to loops of semiconductor junctions with an exponential *V-I* relation. A TL loop is characterised by a certain number of forward-biased PN junctions, the sum of the junction voltages in the loop equates to zero.

$$\sum_{n=1}^{N} V_{jn} = 0, \tag{3.2.4}$$

where V_{jn} is the voltage across junction n.
Using equation (3.2.3), this becomes:

$$\sum_{n=1}^{N} \ln\left(\frac{I_{jn}}{A_n \cdot J_S}\right) = 0, \tag{3.2.5}$$

where I_{jn} is the current passing through junction n,

A_n is the junction area, and

$J_S = J_S(T)_n$ is the reverse saturation current density of junction n.

Since the sum-of-logs to product-of-arguments perperty of logarithms, equation (3.2.5) can also be rewritten as:

$$\prod_{n=1}^{N}\left(\frac{I_{jn}}{A_n \cdot J_S}\right) = 1, \tag{3.2.6}$$

Note that any practical circuit will operate with $I_j >> I_S$, where I_S the reverse saturation current of junction n (i.e., $I_S = A_n J_S$). For example, even at I_j = 100 pA, the ratio of I_j to I_S is typically greater than 10,000 [20]. Thus, for the product of equation (3.2.6) to be unity and sensible current ratios to be maintained, two conditions must be met:

(1). There must be an even number of junctions in a loop;

(2). Half of the junctions must conduct in a clockwise direction and the other half

conduct in a counter-clockwise direction.

Thus, for a general loop:

$$\sum_{n=1}^{N/2} V_{jn} = \sum_{n=N/2+1}^{N} V_{jn}, \tag{3.2.7}$$

or, in a less formal notation:

$$\sum_{CW} V_{jn} = \sum_{CCW} V_{jn}, \tag{3.2.8}$$

where CW is clockwise, and CCW is counter-clockwise.

Plugging equation (3.2.3) into (3.2.8), we obtain:

$$\frac{mkT}{q}\sum_{CW}\ln\left(\frac{I_{jn}}{A_n \cdot J_S}\right) = \frac{mkT}{q}\sum_{CCW}\ln\left(\frac{I_{jn}}{A_n \cdot J_S}\right). \tag{3.2.9}$$

After eliminating the common terms from both sides, we get the *static translinear principle*:

$$\prod_{CW} I_{jn} = \lambda \prod_{CCW} I_{jn}, \tag{3.2.10}$$

where J_S is equal for all transistors, owing to the identical operating temperature, and $\lambda = \prod_{CW} A_n \Big/ \prod_{CCW} A_n$, usually be intentionally designed to be unity, and this assumption is used for noise analysis in next chapter.

An example of four-transistor TL loop is shown in Figure 3.3. It is assumed that the transistors are somehow biased at the collector current I_1 through I_4. So,

$$V_{BE1} + V_{BE3} = V_{BE2} + V_{BE4}. \tag{3.2.11}$$

Following the manipulation from equations (3.2.4) to (3.2.10), equation (3.2.11) yields:

$$I_1 I_3 = \lambda \cdot I_2 I_4, \tag{3.2.12}$$

where $\lambda = A_1 A_3 / A_2 A_4$ is the equivalent area ratio of the TL loop.

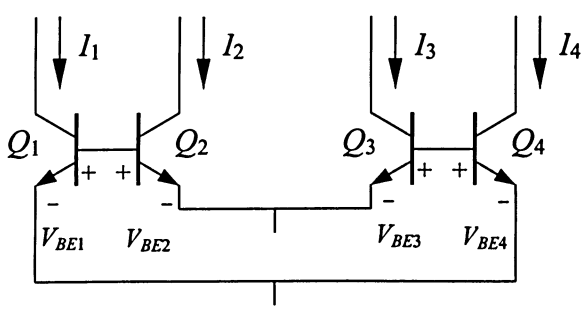

Figure 3.3 A four-transistor translinear loop

Equation (3.2.10) shows that the STL principle can be used to implement the arithmetic operations of multiplication and division. The operations of addition and subtraction are

easily implemented in the current-domain. Thus, using translinear circuits, a wide variety of polynomial functions can be implemented.

In addition, we can find another major advantage of translinear circuit, directly through equation (3.2.10): All temperature-dependent and process-dependent constants, i.e., U_T and I_S, are eliminated. As a consequence, the transfer function implemented by a STL circuit is theoretically termperature and process independent.

Furthermore, it is implemented using such a simple circuit, as shown in Figure 3.3. Thus, TL circuits are characterised by a very high functional density.

3.2.2 Dynamic Translinear Principle

In contrast to STL principle which is limited to frequency-independent transfer functions, by admitting capacitors into the TL loops, the term *Dynamic Translinear* (DTL) was coined by Mulder *et al.* in [14] to describe the circuit that has frequency-dependent transfer functions.

To better understand its behaviour, let us take a current mirror circuit as an example, shown in Figure 3.4.

In this circuit, a capacitor C is connected in parallel with the diode-connected input transistor. The capacitor can be regarded as the internal integrator and the output transistor as the expander of a companding system [10], as shown as Figrure 3.2. The current mirror is biased in class A by a DC bias current I_{dc}, the AC input current I_{in} is superimposed on I_{dc}.

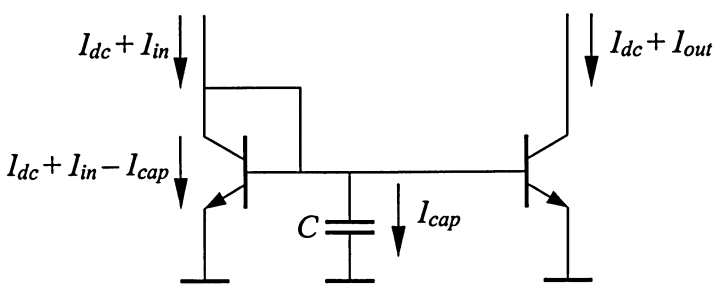

Figure 3.4 A capacitor added to a current mirror

For very small values of I_{in}, the transconductance g_m of each of the two transistors is approximately constant. In that case, the transfer function from the capacitance voltage

swing to the AC output current I_{out} is linear. Consequently, we get the transfer function in the form of a linear DE [12]:

$$\frac{CU_T}{I_{dc}}\dot{I}_{out} + I_{out} = I_{in}. \tag{3.2.13}$$

For relatively large input signal swings, g_m of the output transistor is no longer a constant. Therefore, a general non-linear DE is given by:

$$\frac{CU_T}{I_{dc} + I_{out}}\dot{I}_{out} + I_{out} = I_{in}. \tag{3.2.14}$$

Figure 3.5 shows the simulation of the transfer function of the current mirror. In the simulation, I_{dc} is 50 μA and C is 300 pF.

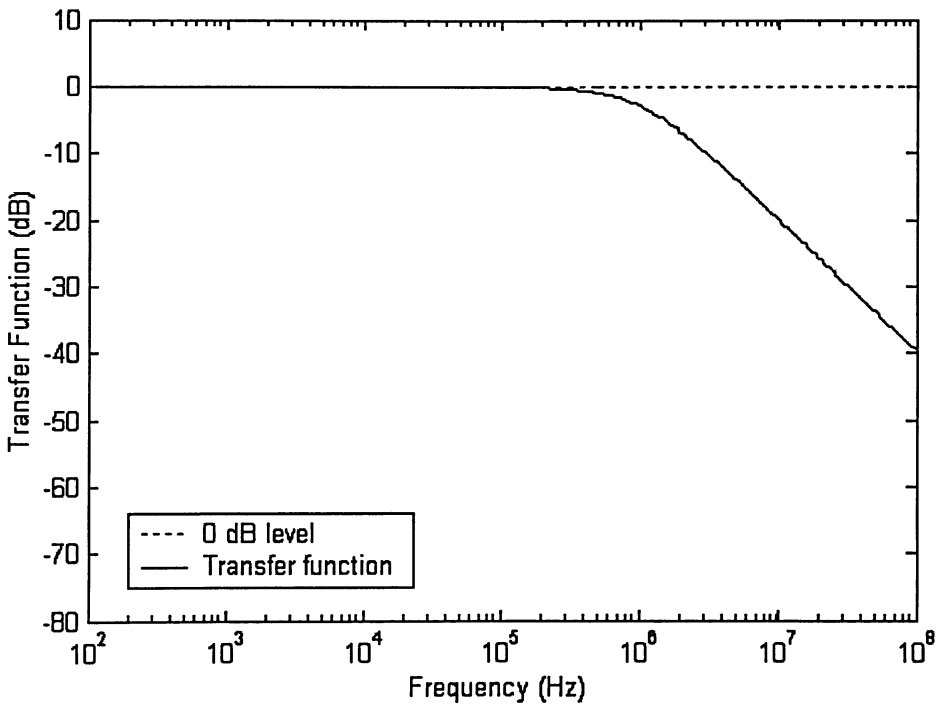

Figure 3.5 Simulation of transfer function of current mirror

We know, the exponential function has two favourable characteristics. First, the multiplication of two exponential functions e^a and e^b is equivalent to addition of the two arguments a and b, $e^a \cdot e^b = e^{a+b}$. Second, the derivative of an exponential function equals itself. The first characteristic is exploited in the STL principle, while the second one is the basis of the DTL principle.

From equation (3.2.1), we calculate the derivative of I_C with respect to time, the result is:

$$\dot{I}_C = I_C \frac{\dot{V}_{BE}}{U_T}. \tag{3.2.15}$$

The relation between capacitance current I_{cap} and its voltage V_{cap} is given by:

$$I_{cap} = C\dot{V}_{cap} = C\dot{V}_{BE}. \tag{3.2.16}$$

Combining equation (3.2.15) and (3.2.16), we get:

$$CU_T\dot{I}_C = I_C \cdot C\dot{V}_{BE} = I_C \cdot I_{cap}.$$

Hence,
$$I_{cap} = CU_T \frac{\dot{I}_C}{I_C}, \tag{3.2.17}$$

i.e.,
$$\dot{I}_C = \frac{1}{CU_T} I_C \cdot I_{cap}, \tag{3.2.18}$$

where the dimension is [A]. This is illustrated in Figure 3.6.

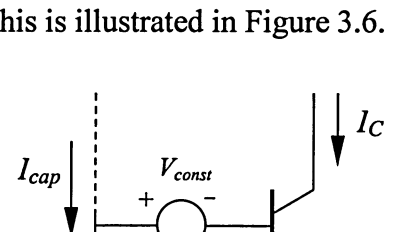

Figure 3.6 Principle of dynamic translinear circuit

Hence comes the DTL principle [14]: "A time derivative of a current is equivalent to a product of currents". Using this principle, the product of currents on the right-hand-side of equation (3.2.17) can be realised very elegantly. The structure is shown in Figure 3.6, which is typical for the class of log-domain filters. In other words, the derivative is equivalent to the product of a capacitor current and one collector current.

The DTL principle can be used to implement DEs, and hence a wide variety of signal processing functions. For example, linear DEs can be used for filters, and non-linear DEs can be used for harmonic and chaotic oscillators, PLLs and RMS-DC converters [14].

Chapter 4

Noise Analysis Methods for Translinear Circuits

In this chapter, we will analyze noise sources and their effects upon translinear circuits.

Noise is an important non-ideal aspect in most electronic circuits. Translinear circuits are an externally linear but internally non-linear circuits. Therefore, the noise analysis is of fundamental importance. Furthermore, static translinear circuits do not have a perticularly good reputation in terms of noise, and it is likely that dynamic translinear circuits inherit these noise characteristics.

In Section 4.1, two important measures for describing the noise behaviour of analogue circuits, the dynamic range (DR) and the maximum signal-to-noise ratio (SNR) are defined to clarify later analyses.

Several important internal noise sources are discussed in Section 4.2. These noises primarily come from transistors, and are modulated by signals being processed. Thus, the situation is very complicated.

Because the noise in TL circuits is non-linear and non-stationary, Section 4.3 discusses the basic noise analysis methods, and then Sections 4.4 and 4.5 provide non-linear noise analysis methods based on non-linear signal processing theory.

4.1 Dynamic Range and Signal-to-Nosie Ratio

To clarify the discussion, the two measures, DR and SNR, are defined here:

- The DR equals the ratio of of the maximum signal power to the minimum acceptable signal power. Here, the minimum acceptable signal power is equal to the noise power in the absence of signals [11].

- The (maximum) SNR equals the (maximum) ratio of the signal power to the noise power at the same time [12].

From the above two definitions, for a number of conventional amplifers and filters based on linear circuit elements, DR and maximum SNR are equal, since the noise floor is constant.

However, in translinear circuits, or companding filters in general, due to signal-noise intermodulation, the maximum SNR can be much smaller than DR [15]. That is to say, the non-stationary noise and signal-noise intermodulation make the equivalent input noise spectrum to be time-dependent.

Hence, the easiest way to define SNR of a circuit with a non-stationary noise spectrum is to give a stationary interpretation to the noise spectrum. A logic and practical way is to use the average noise spectrum to define SNR.

4.2 Transistor Noise Sources

4.2.1 Noise Sources

The noise behaviour of bipolar transistors is characterized mainly by four statistically independent noise sources.

First, the collector shot noise can be represented by a current shot noise source i_C, connected between the collector and emitter terminals. The power spectral density function S_{i_C} is flat since it is a white noise, referred to the description in Chapter 2:

$$S_{i_C}(\omega,t) = 2qI_C(t). \qquad (4.2.1)$$

Second, the base shot noise is represented by a noise current source i_B connected between the base and emitter terminals. Its power spectral density function S_{i_B} is also white, and equals

$$S_{i_B}(\omega,t) = 2qI_B(t). \qquad (4.2.2)$$

Third, the flicker noise, or $1/f$ noise, is the product of a process-dependent noise mechanism, is also represented by a noise source between the base and emitter terminals. For DC base currents, the power spectral density of this noise is given by

$$S_{i_{Bf}}(\omega,t) = 2qf_l\frac{I_B}{f} = 2qI_B\frac{2\pi f_l}{\omega}, \qquad (4.2.3)$$

where the constant $K = 2qf_l$, is a physical factor due to contamination and crystal

imperfections. For details, please referred to Section 2.3. Here, f_l is a frequency at which it equals the base shot noise spectral density, shown in equation (4.2.2).

The last noise source is the thermal base resistance noise source v_{R_B}, generated by the base resistance R_B of bipolar transistors, having a white power spectral density

$$S_{R_B}(\omega) = 4kTR_B. \tag{4.2.4}$$

Since we prefer to the current-mode approach, we need to transform the noise voltage v_{R_B} to a noise current source i_{R_B} connected in parallel with i_C. As we know, $v_{R_B} << U_T$, the small-signal transconductance $g_m = I_C / U_T$ can be used for this transformation.

$$\begin{aligned} S_{iR_B}(\omega,t) &= g_m^2 \cdot S_{R_B}(\omega) = \frac{I_C^2(t)}{U_T^2} 4kTR_B = \frac{I_C^2(t)}{U_T \cdot kT/q} 4kTR_B \\ &= (2qI_C(t)) \frac{2R_B I_C(t)}{U_T} = S_{i_C}(\omega,t) \frac{2R_B I_C(t)}{U_T}. \end{aligned} \tag{4.2.5}$$

In traditional noise analysis, the collector and base currents are usually approximated as being DC currents. All corresponding noise sources are thus stationary. However, this approximation is not accurate for TL circuits, where the transistor currents are often strongly signal-dependent. Therefore, the shot noise sources in a TL circuit are principally non-stationary. This explains why the time variable t exists in equations (4.2.1) through (4.2.5).

4.2.2 Comparison Among the Noise Sources

Assume noise sources are uncorrelated to each other, the equivalent noise current power spectral density of a transistor at the collector node is:

$$S_{i_{C\_total}}(\omega,t) = S_{i_C}(\omega,t) + S_{i_B}(\omega,t) + S_{i_{Bf}}(\omega,t) + S_{iR_B}(\omega,t). \tag{4.2.6}$$

By comparing the noise sources, it is possible to determine their relative influence in TL circuits. From equations (4.2.6), all the noise sources are elegantly described in terms of currents, either I_C or I_B, so we can compare them directly.

In translinear circuits, the transistors are forced to use either diode-like connections or amplifier implementations, as illustrated in Figure 4.1.

In translinear circuits, the influence of the base shot noise is often negligible in

comparing with the collector shot noise. This can be evaluated as follows.

In a diode connected transistor, shown in Figure 4.1(a), i_C and i_B are connected in parallel. And we know the noise power of i_B is β_F^2 times smaller than that of i_C, thus it is negligible for sufficiently large values of β_F. If an amplifier is used to force the collector current, shown in Figure 4.1(b), the influence of i_B is further decreased. The noise source i_B is divided by the current gain G of the amplifier when transformed to the collector terminal. This amplifier is often implemented by a common-collector stage, which possibly is another transistor in the TL loop, thus having a double functionality [11].

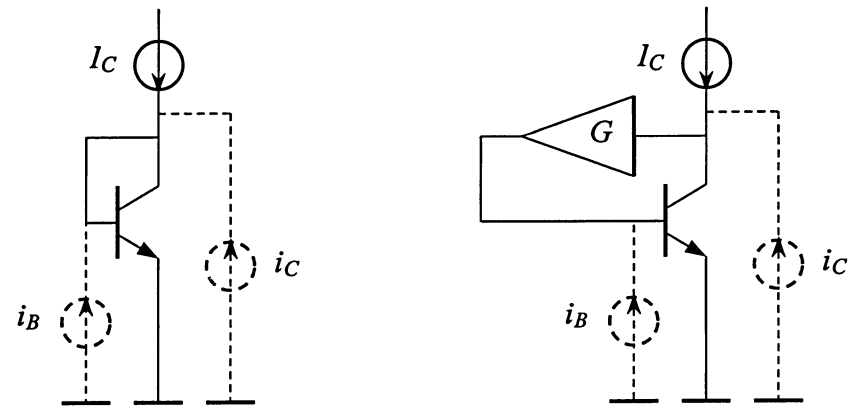

(a) A diode connection (b) An amplifier connection

Figure 4.1 Biasing of a transistor in translinear circuit

The flicker noise is characterised by the corner frequency f_l . In common bipolar I_C processes, f_l is usually quite low, typically a few hertz, and decreases when the base current decreases [20]. Due to the very small influence of base current shot noise in TL circuits, the relative influence of $1/f$ noise in a TL circuit is characterised by a much lower corner frequency of about f_l /β_F. As a consequence, the flicker noise can be safely neglected in most applications.

The thermal noise generated by the base resistance cannot be compared directly to the shot noise sources. The noise voltage v_{R_B} need to be transformed to an equivalent noise current source. Note in principle, this transformation of v_{R_B} yields two components: a noise current source between the collector and emitter terminals, and a noise voltage source in series with the collector terminal. However, the influence of the latter on the collector current is negligible, because of high transistor output impedance [21].

Referring to equations (4.2.1) and (4.2.5), we can conclude that S_{iR_B} is negligible when it

is much smaller than S_{i_C} at low current levels, i.e., $I_C << \frac{1}{2}U_T/R_B$. The higher the current level, the heavier influence the thermal noise. At high current levels, i.e., $I_C >> \frac{1}{2}U_T/R_B$, v_{R_B} becomes the dominant source of noise.

Hence, when we analyze the noise influence in TL circuits, we can neglect base shot noise and flicker noise, thus the total noise formula can be simplified to:

$$\begin{aligned} S_{total}(\omega,t) &= S_{i_C}(\omega,t) + S_{iR_B}(\omega,t) \\ &= S_{i_C}(\omega,t)\left(1+\frac{2R_B I_C(t)}{U_T}\right). \end{aligned} \tag{4.2.7}$$

4.2.3 Signal-to-Noise Ratio

An indication of the maximal SNR of a TL circuit can be derived from the SNR of a single bipolar transistor.

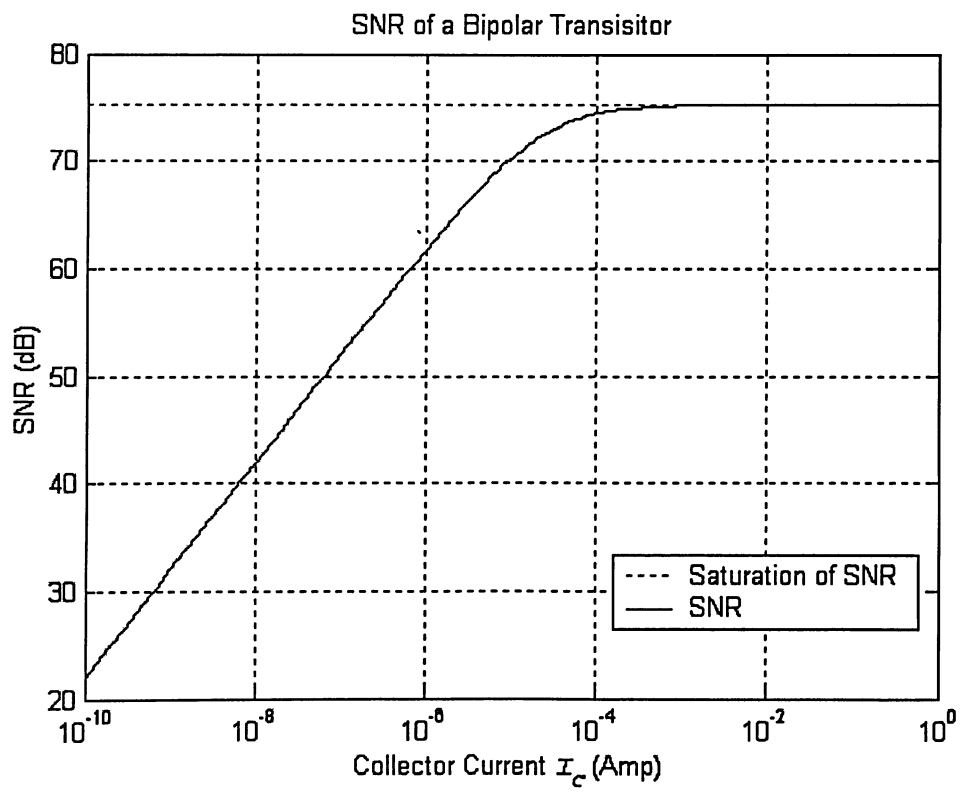

Figure 4.2 The SNR of a bipolar transistor

The signal power processed by a single transistor is proportional to the square of I_C. For simplicity, here, we regard the DC value of I_C as being the processed signal, thus all noise

sources becomes stationary. Dividing this by the noise power in an equivalent noise bandwidth B (in hertz), the SNR of a single bipolar transistor is given by:

$$SNR = \frac{I_C^2}{2qI_C(1+2R_BI_C/U_T)2B} = \frac{I_C}{4qB(1+2R_BI_C/U_T)}, \qquad (4.2.8)$$

and we can easily get the saturation level of SNR:

$$\lim_{I_C \to \infty} SNR = \frac{U_T}{8qBR_B}. \qquad (4.2.9)$$

A TL circuits consists of one or more TL loops. Each of these loops can more or less be regarded as being a cascade of transistors. The SNR of such a loop is thus limited by the transistor that has the lowest SNR and the equivalent noise bandwidth.

For example, given R_B = 600 Ω, and B = 1 MHz, the SNR increases linearly proportional to I_C (due to i_C), and saturates to 75.3 dB, due to i_{R_B}, as illustrated in Figure 4.2.

4.3 Noise Analysis Method

Due to the exponential relation between V_{BE} and I_C of transistors, translinear circuits behave non-linearly. Basically, there are four major non-linear behaviours, all from exponential device characteristics.

First, the multiplication of collector currents, see equation (3.2.9), introduces signal-noise intermodulation. Second, the signal-dependent transformation of the base resistance thermal noise voltage source into noise current source also introduces multiplicative non-linearity, see equation (4.2.5). Third, due to the time-various collector currents, the noise current sources are, in general, non-stationary. Finally, in dynamic translinear circuits, the inclusion of capacitors results in nonlinear dynamic transfer functions.

Therefore, the objective of nonlinear noise analysis methods is to acquire an equivalent output noise characteristic, due to internal noise production.

4.3.1 TL Equations with Noise

This is the first step, to include the noise sources in TL equations. For this purpose, the main noise sources are added to each transistor. For example, Figure 4.3 depicts the

inclusion of collector shot noise current sources and base resistance thermal noise voltage sources, in the second-order TL loop of Figure 3.3. Transistors are biased at currents I_1 through I_4. Each transistor is accompanied with a shot noise source, from i_1 through i_4, and a thermal noise voltage source, v_5 through v_8. Because we prefer current sources, these voltage sources need to be converted to the equivalent current sources through equation (4.2.5).

Since the junctions in a TL loop are serially connected, v_5 to v_8 can be combined into a single noise source v_R, and therefore i_R, in current mode. As a result, it can move freely through the TL loop [11].

From the translinear circuit principle in equation (3.2.10), with $\lambda = 1$ (for simplicity), we get the TL loop equation including noise sources i_1 through i_4:

$$(I_1 + i_1)(I_3 + i_3) - (I_2 + i_2)(I_4 + i_4) = 0. \qquad (4.3.1)$$

Since the equation contains both signals and noises, it becomes the basis of non-linear noise analysis.

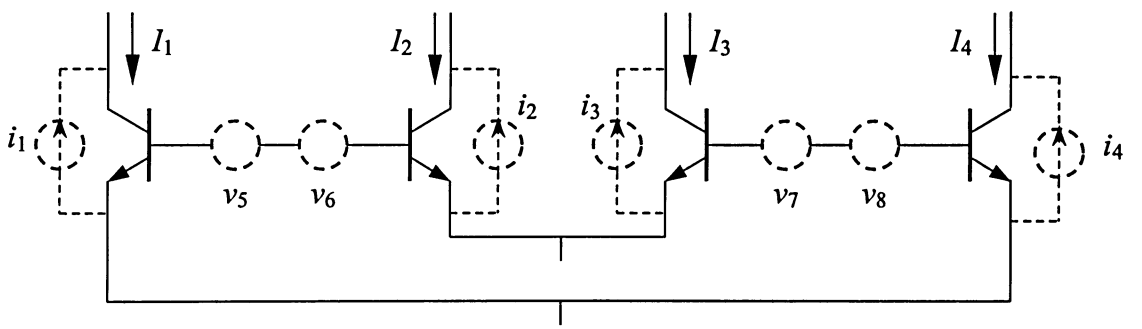

Figure 4.3 Translinear loop in the presence of noise

4.3.2 Input-Output Equation with First-Order Noise

This step is to figure out the input-output relation, including the influence of noise. Elaborating equation (4.3.1), we get

$$I_1 I_3 + I_1 i_3 + I_3 i_1 + i_1 i_3 - I_2 I_4 - I_2 i_4 - I_4 i_2 - i_2 i_4 = 0. \qquad (4.3.2)$$

In general, an nth-order polynomial is obtained for an nth-order TL loop. In this equation, each term comprises the products of signal and/or noise currents. As long as the noise is generally much smaller than the signals, products of two noise currents are small enough

to be ignored [29]. Therefore, only products that have at most one noise current remain, i.e., first-order noise or signal-noise intermodulation, are relevant. This yields:

$$I_1 I_3 + I_1 i_3 + I_3 i_1 - I_2 I_4 - I_2 i_4 - I_4 i_2 = 0. \tag{4.3.3}$$

It is interesting that from equation (4.3.3), noise sources show no mutual influence. Therefore, they are uncorrelated and can be calculated individually.

The input-output relation can be solved by rearranging the expression of the above equation (4.3.3). The output current I_{out}, which is one of the currents I_n, n=1,2,3,4, can be expressed by the input current I_{in} and the noise current i_n. Thus, the result is a polynomial, a rational function or a function containing nth-order roots.

Because noise is usually much smaller than signals, first-order noise components thus can provide sufficient accuracy. So, the output I_{out} can be approximately expressed through the first-order Taylor series, as a function of I_{in} and all first-order noise and signal-noise components.

4.3.3 Autocorrelation and Power Spectral Density

Autocorrelation and power spectral density (PSD) are two important indicators to determine the noise influence.

It is natural to divide the output current I_{out} into three mutually uncorrelated components. Denote $\vec{s}(t)$ as the input signal vector, $\vec{n}(t)$ as the noise sources vector of all noise currents i_n. So, $\vec{n}(t)$ is statistically dependent on $\vec{s}(t)$ when it contains shot noise. So, the first component is the noise-free part, a deterministic component $C(t)$:

$$C(t) = E[I_{out}(t)]_{\vec{s},\vec{n}}, \tag{4.3.4a}$$

the second one is the signal component $S(t)$:

$$S(t) = E[I_{out}(t)|\vec{s}(t)]_{\vec{n}} - C(t), \tag{4.3.4b}$$

the last part is the total noise component $T(t)$:

$$T(t) = I_{out}(t) - C(t) - S(t), \tag{4.3.4c}$$

where $E[\cdot]$ represents the statistical expectation, i.e., the ensemble average at a certain time t, with respect to $\vec{s}(t)$ and/or $\vec{n}(t)$, as denoted by the indices. The signals $C(t)$, $S(t)$ and $T(t)$ are completely uncorrelated. Hence, the autocorrelation functions $R_C(\tau, t)$, $R_S(\tau, t)$ and $R_T(\tau, t)$, and the power spectral density $S_C(\omega, t)$, $S_S(\omega, t)$ and $S_T(\omega, t)$ can be computed separately and directly. At last, by combining these components, we can obtain the autocorrelation of I_{out}, $R_{Iout}(\tau, t)$, and its Fourier transform to τ, PSD $S_{Iout}(\omega, t)$.

The noise component $T(t)$ can be further separated into a signal-independent noise and a signal-dependent noise. So, based on first-order Taylor approximation, each noise source $T_i(t)$ can be expressed by a noise current source $i_i(t)$ and a noise-free signal current $G_i(t)$ [29], where subscription i stands for one of the n noise sources:

$$T_i(t) = i_i(t) \cdot G_i(t), \tag{4.3.5}$$

For non-stationary collector shot noise, it is convenient to represent it as a modulated stationary noise source, i.e.:

$$i_C(t) = a(t) \cdot n(t), \tag{4.3.6}$$

where $n(t)$ is a stationary noise source and $a(t)$ is the modulation function. By definition, the power spectral density of $n(t)$ is:

$$S_n(\omega) = 2qI_o, \tag{4.3.7}$$

where I_o is a dc current, then the modulation function $a(t)$ can be drived from:

$$\sqrt{2qI_C(t)} = a(t)\sqrt{2qI_o},$$

i.e.,

$$a(t) = \sqrt{I_C(t)/I_o} \tag{4.3.8}$$

Often, the noise $i_i(t)$ is a shot noise, the autocorrelation of $R_{Ti}(\tau, t)$ can be calculated as:

$$\because \quad T_i(t) = i_i(t) \cdot G_i(t) = n_i(t)a_i(t)G_i(t),$$

$$\therefore \quad R_{T_i}(\tau, t) = R_{T_i}(\tau) \cdot [a_i(t)G_i(t)]^2, \tag{4.3.9}$$

Similarly, the power spectral density function $S_{Ti}(\omega, t)$ of $R_{Ti}(\tau, t)$ is:

$$\begin{aligned} S_{T_i}(\omega, t) &= S_{T_i}(\omega) \cdot [a_i(t)G_i(t)]^2 \\ &= 2qI_{C_i}(t)G_i(t)^2 \end{aligned} \tag{4.3.10}$$

In the above discussion, thermal noise sources are omitted. As mentioned before, the thermal noise source v_n can be converted to the quivalent current source i_n, thus dpendent on collector current $I_C(t)$, and it can be shifted freely through the TL loop [12]. Obviously, it is the simplest choice to select a transistor that is biased at a constant current. This is a prevalent situation.

4.3.4 Output SNR

Finally, the circuit output SNR for a given input signal is ready for determination. Intuitively, both the signal power and the noise power should be independent of time. However, when the input signals are nonstationary, the noise power obtained by integration of equation (4.3.10) over ω is time-dependent:

$$P_T(t) = \int_{-B}^{B} S_T(\omega, t) d\omega . \tag{4.3.11}$$

A convenient way to reach the time-independent SNR is to average the power, or equivalently the power spectral density, over time,

$$P_T = E[P_T(t)]. \tag{4.3.12}$$

Therefore, we can obtain the final time-independent SNR:

$$SNR = \frac{P_{sig}}{P_T}. \tag{4.3.13}$$

4.4 Noise in Static Translinear Circuits

In this section, we will apply the proposed noise analysis method to some generic static translinear circuits.

We will firstly analyze a very simple circuit, the current mirror, which has been mentioned in section 3.2.2. Consequently, some circuits containing second-order TL loop, a square circuit and a square-root circuit, are discussed.

4.4.1 Current Mirror

Current mirror is the simplest translinear circuit. In this circuit, Q_1 and Q_2 are identical. Therefore, the parameter λ in the equation (3.2.9) becomes 1. In general, TL circuits are described by products of currents. However, in this case, the circuit is too simple to have current multiplications. It shows to be a first-order polynomial. The only mechanism of signal-noise intermodulation occurs at the transformation of the noise voltage v_{R_B} into an equivalent noise current i_{R_B}.

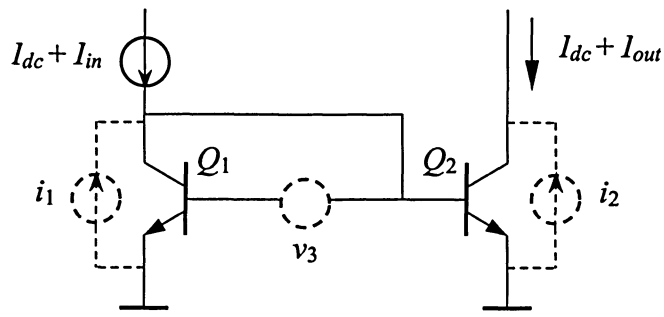

Figure 4.4 A current mirror with noise sources

Figure 4.4 shows a two-transistor current mirror. The dc current I_{dc} is greater than the peak value of I_{in}, resulting in $I_{dc}+I_{in}>0$ all the time. This is so-called class A biasing. I_{in} is a zero-mean current.

Three noise sources i_1, i_2, and v_3 are depicted, where v_3 represents the sum of the two thermal noise sources of Q_1 and Q_2 [12].

First, the voltage source v_3 need to be transformed to an equvialent noise current source i_3, which is in parallel with i_1. We know the transconductance g_{m_1} of Q_1 is I_{C_1}/U_T, where $I_{C_1}=I_{dc}+I_{in}$. Therefore, i_3 is found to be:

$$i_3 = g_{m_1} v_3 = (I_{dc} + I_{in})\frac{v_3}{U_T}. \tag{4.4.1}$$

From equation (4.4.1), we can clearly see the signal-noise intermodulation. The noise source i_3 contains two uncorrelated parts. The first part is $I_{dc}\, v_3/U_T$, only depended on the statistics of v_3. However, the second part, $I_{in}\, v_3/U_T$, is the intermodulation of signal I_{in} and noise v_3.

Neglecting all non-idealities of the circuit, based on the TL principle shown in equation (3.2.9), the collector currents of Q_1 and Q_2 are equal, i.e.,

$$I_1 = I_2. \tag{4.4.2}$$

Then, we add non-idealities into the equation (4.4.2). As mentioned before, thermal noise source v_3 can move freely in the circuit, we thus associate it with Q_1. Therefore, we obtain:

$$\begin{aligned} I_{dc} + I_{in} + i_1 + i_3 &= I_{dc} + I_{out} + i_2 \\ I_{out} &= I_{in} + i_1 + i_3 - i_2 \\ &= I_{in} + i_1 - i_2 + (I_{dc} + I_{in})\frac{v_3}{U_T} \end{aligned} \tag{4.4.3}$$

Applying the noise analysis method in the previous section to this equation, using principle equations (4.3.4a) – (4.3.4c), it is easy to match them to:

$$C = 0, \tag{4.4.4a}$$

$$S(t) = I_{in}, \tag{4.4.4b}$$

$$T(t) = i_1 - i_2 + (I_{dc} + I_{in})\frac{v_3}{U_T}. \tag{4.4.4c}$$

In this circuit, all noise sources are assumed to be uncorrelated. So, the autocorrelation of the total output noise $T(t)$ is:

$$R_T(\tau,t) = R_{i_1}(\tau,t) + R_{i_2}(\tau,t) + R_{v_3}(\tau,t)\left[\frac{(I_{dc}+I_{in})}{U_T}\right]^2, \tag{4.4.5}$$

R_{i1} and R_{i2} are shot noises, equal to $2qI_C(t)\delta(t)$. Applying Fouier transform to (4.4.5), the corresponding time-dependent power spectral density is:

$$\begin{aligned} S_T(\omega,t) &= S_{i_1}(\omega,t) + S_{i_2}(\omega,t) + S_{v_3}(\omega,t)\left[\frac{(I_{dc}+I_{in}(t))}{U_T}\right]^2 \\ &= 2q(I_{dc}+I_{in}(t)) + 2q(I_{dc}+I_{in}(t)) + 4kTR_B\left[\frac{(I_{dc}+I_{in}(t))}{U_T}\right]^2 \end{aligned} \tag{4.4.6}$$

Because we are expecting the time-independent PSD, we need to find the expectation over a stationary input $I_{in}(t)$. To this end, let it be a sine wave at frequency ω_0:

$$I_{in} = mI_{dc}\sin(\omega_0 t + \phi), \tag{4.4.7}$$

where m is the modulation index, and ϕ is a uniformly distributed stochastic variable, representing the arbitrary choice of the origin of the time axis. Then the ensemble average of $S_T(\omega)$ is:

$$\begin{aligned} \overline{S_T(\omega)} &= E[S_T(\omega,t)] \\ &= 2qI_{dc} + 2qI_{dc} + \frac{4qR_B}{U_T}\overline{(I_{dc}+I_{in})^2} \\ &= 2qI_{dc} + 2qI_{dc} + \frac{4qR_B}{U_T}\left[I_{dc}^2 + \overline{I_{in}^2} + 2I_{dc}\overline{I_{in}}\right] \\ &= 4qI_{dc} + \frac{4qR_B}{U_T}\left[I_{dc}^2 + \frac{1}{2}m^2 I_{dc}^2\right] \\ &= 4qI_{dc}\left[1 + \frac{R_B I_{dc}}{U_T}\left(1+\frac{1}{2}m^2\right)\right], \end{aligned} \tag{4.4.8}$$

where $\overline{I_{in}} = mI_{dc}\cdot\frac{\omega_0}{2\pi}\int_0^{2\pi/\omega_0}\sin(\omega_0 t+\phi)dt = 0$, since it is a zero mean signal,

$\overline{I_{in}^2} = m^2 I_{dc}^2\cdot\frac{\omega_0}{2\pi}\int_0^{2\pi/\omega_0}\sin^2(\omega_0 t+\phi)dt = m^2 I_{dc}^2\cdot\frac{1}{2}$.

Applying the equations described in Section 4.3.4, we can get the SNR of the circuit:

$$\begin{aligned} SNR &= \frac{P_{signal}}{P_{noise}} = \frac{\frac{1}{2}m^2 I_{dc}^2}{2B\cdot 4qI_{dc}\left[1+\frac{R_B I_{dc}}{U_T}\left(1+\frac{1}{2}m^2\right)\right]} \\ &= \frac{m^2}{16qB\left[\frac{1}{I_{dc}}+\frac{R_B}{U_T}\left(1+\frac{1}{2}m^2\right)\right]}. \end{aligned} \tag{4.4.9}$$

The saturation level follows from the asymptote:

$$\lim_{I_{dc}\to\infty} SNR = \frac{U_T m^2}{8qR_B B(2+m^2)}. \tag{4.4.10}$$

Figure 4.5 shows a simulation of the SNR vs. dc current in a current mirror, where R_B = 600 Ω, and B = 1 MHz. When I_{dc} is small, i.e., $I_{dc} << \frac{U_T}{R_B(1+m^2/2)}$, the resistance thermal noise is negligible, the SNR is linearly increasing subject to I_{dc}. However, when I_{dc} is relatively high, the SNR is almost the same as saturation level.

In addition, the saturation level of SNR is a function of the modulation index m, thus, various m can lead to different noise influence.

Note, because this circuit works in class A, m is always less than 1. In other words, the input current is always positive.

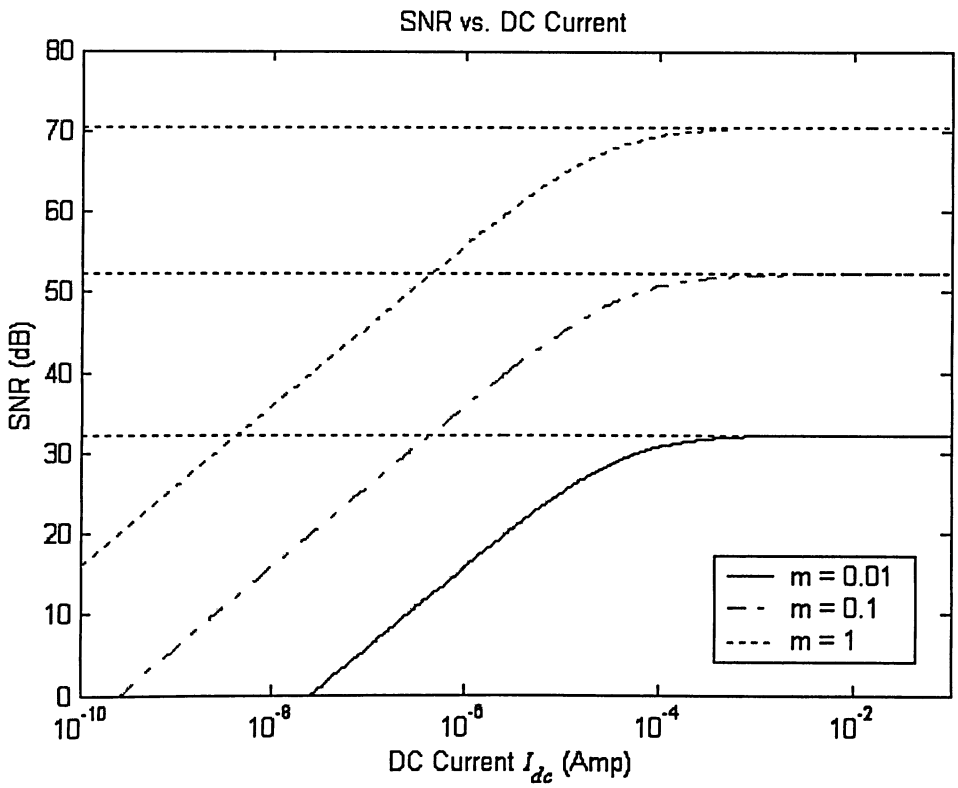

Figure 4.5 Signal-to-noise ratio for current mirror

4.4.2 Square Circuit

Now, consider a frequency doubler, using a square circuit shown in Figure 4.6. Similar to the previous simple current mirror, all four transistors contribute their shot noise sources i_1 through i_4, and four base resistance thermal noise sources are combined into one source v_5 [12]. The input signal I_{in} is biased by a dc current I_{dc}, so that the collector currents of transistors Q_1 and Q_2 consist of both above currents.

Q_3 is biased at I_o, a constant dc current, thus v_5 can be transformed to an equivalent noise current source in parallel with i_3, without introducing signal-noise intermodulation. To simplify the equations, and without lossing generality, v_5 will be assumed to be negligible. Thus, the TL loop equation is:

$$(I_{dc}+I_{in}+i_1)(I_{dc}+I_{in}+i_2)=(I_o+i_3)(I_{out}+i_4), \tag{4.4.11}$$

By rearranging the equation (4.4.11), eliminating second-order noise terms, we obtain:

$$I_{out}=\frac{(I_{dc}+I_{in}+i_1)(I_{dc}+I_{in}+i_2)}{(I_o+i_3)}-i_4. \tag{4.4.12}$$

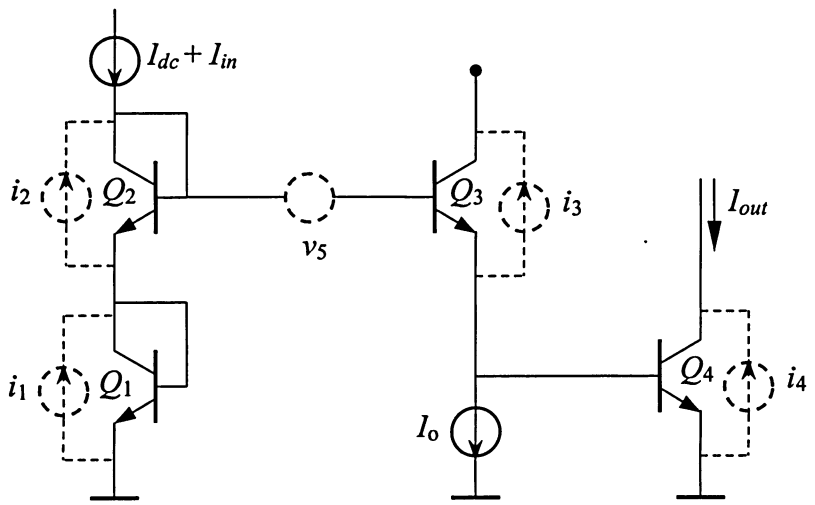

Figure 4.6 TL square circuit with noise sources

Since $(I_o+i_3)(I_o-i_3)=I_o^2-i_3^2\cong I_o^2$, i.e.,

$$(I_o+i_3)\cong\frac{I_o^2}{(I_o-i_3)}, \tag{4.4.13}$$

plugging equation (4.4.13) into (4.4.12), and ignoring second-order noises,

$$I_{out} = (I_o - i_3)\frac{(I_{dc}+I_{in})^2}{I_o^2} + \frac{(i_1+i_2)(I_{dc}+I_{in})}{I_o} - i_4$$
$$= \frac{(I_{dc}+I_{in})^2}{I_o} + \frac{(I_{dc}+I_{in})}{I_o}(i_1+i_2) - i_3\frac{(I_{dc}+I_{in})^2}{I_o^2} - i_4 \qquad (4.4.14)$$

Applying noise analysis equations (4.3.4a) – (4.3.4c),

$$C(t)+S(t) = \frac{(I_{dc}+I_{in})^2}{I_o}, \qquad (4.4.15)$$

and

$$T(t) = (i_1+i_2)\frac{(I_{dc}+I_{in})}{I_o} - i_3\frac{(I_{dc}+I_{in})^2}{I_o^2} - i_4. \qquad (4.4.16)$$

Assume the input signal $I_{in} = mI_{dc}\sin(\omega_0 t+\phi)$, same as (4.4.7) in preivous section, equation (4.4.15) can be split into:

$$C(t)+S(t) = \frac{[I_{dc}+mI_{dc}\sin(\omega_0 t+\phi)]^2}{I_o}$$
$$= \frac{I_{dc}^2}{I_o}[1+2m\sin(\omega_0 t+\phi)+m^2\sin^2(\omega_0 t+\phi)]$$
$$= \frac{I_{dc}^2}{I_o}\left[1+2m\sin(\omega_0 t+\phi)+m^2\frac{1-\cos(2\omega_0 t+2\phi)}{2}\right]$$
$$= \frac{I_{dc}^2}{I_o}\left(1+\frac{1}{2}m^2\right)+\frac{mI_{dc}^2}{2I_o}[4\sin(\omega_0 t+\phi)-m\cos(2\omega_0 t+2\phi)]$$

Therefore, $$C = \frac{I_{dc}^2}{I_o}\left(1+\frac{1}{2}m^2\right), \qquad (4.4.17)$$

$$S(t) = \frac{mI_{dc}^2}{2I_o}[4\sin(\omega_0 t+\phi)-m\cos(2\omega_0 t+2\phi)]. \qquad (4.4.18)$$

Equation (4.4.16) reveals that i_1 and i_2 are modulated by the fundamental frequency, whereas i_3 modulated by the second harmonic frequency component. In this circuit, the dc level of the output trnasistor, C, is a function of the modulation index m.

Calculating the autocorrelation functions and then applying Fourier transformations, the power spectral density functions of C, S and T are:

$$S_C(\omega) = 2\pi\left[\frac{I_{dc}^2}{I_o}\left(1+\frac{1}{2}m^2\right)\right]^2\delta(\omega), \qquad (4.4.19a)$$

$$S_S(\omega) = \left[\frac{mI_{dc}^2}{2I_o}\right]^2 \{8\pi[\delta(\omega+\omega_0)+\delta(\omega-\omega_0)] + \tfrac{1}{2}m^2\pi[\delta(\omega+2\omega_0)+\delta(\omega-2\omega_0)]\}, \quad (4.4.19b)$$

$$S_T(\omega,t) = \frac{4q(I_{dc}+I_{in})^3}{I_o^2} + \frac{2q(I_{dc}+I_{in})^4}{I_o^3} + \frac{2q(I_{dc}+I_{in})^2}{I_o}. \quad (4.4.19c)$$

The time-independent noise PSD, can be derived from its ensemble average:

$$\overline{S_T} = \frac{2qI_{dc}^2}{I_o}\left[\left(1+\frac{1}{2}m^2\right)+\frac{I_{dc}}{I_o}\left(2+3m^2\right)+\frac{I_{dc}^2}{8I_o^2}\left(8+24m^2+3m^4\right)\right]. \quad (4.4.20)$$

Set the bandwidth of interest to [-B, B], $B \geq 2\omega_0/\pi$, i.e., bandwidth $2B$ around $2\omega_0$, the SNR can be obtained by dividing the integration of equation (4.4.19b) over integration of (4.4.20):

$$SNR = \frac{I_o}{4qB}\frac{I_{dc}^2 m^2\left(m^2+16\right)}{I_{dc}^2\left(3m^4+24m^2+8\right)+8I_{dc}I_o\left(3m^2+2\right)+4I_o^2\left(m^2+2\right)}. \quad (4.4.21)$$

The saturation level of SNR is calculated as:

$$\lim_{I_{dc}\to\infty} SNR = \frac{I_o}{4qB}\frac{m^2(m^2+16)}{(3m^4+24m^2+8)}, \quad (4.4.22)$$

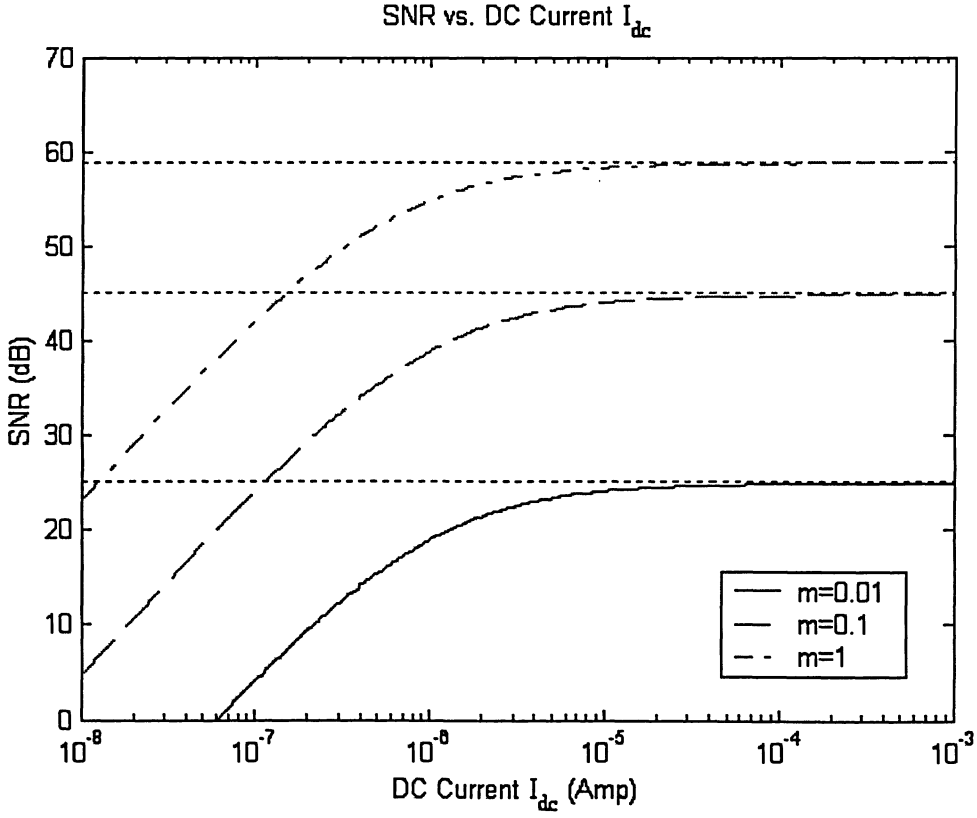

Figure 4.7 Signal-to-Noise ratio for Square Circuit

Why the SNR will be saturated at a certain level? As I_{dc} increases, the power contents of the collector currents through all transistors in the loop, except Q_3, increase. So, the SNR increases as well. However, the collector current of Q_3 remains at the fixed level I_o, and because a TL loop is basically a cascade of transistors, Q_3 will finally limit the SNR of the entire loop.

Figure 4.7 shows the simulation result of the equations (4.4.21) and (4.4.22). The fixed current source I_o = 1 μA, the other parameters are the same as those in current mirror circuit.

To get the optimal value of SNR, we can manipulate the relation between I_o and I_{dc}. Denote $I_o = \lambda I_{dc}$, the equation 4.4.21 can be rewritten as:

$$SNR = \frac{1}{4qB}\frac{m^2(m^2+16)\lambda}{(3m^4+24m^2+8)+8(3m^2+2)\lambda+4(m^2+2)\lambda^2} I_{dc}. \qquad (4.4.23)$$

Denote the SNR to $\eta(\lambda)$, to get the optimal value of SNR, the derivative of $\eta(\lambda)$ with respect to λ should be zero, i.e.,

$$\frac{\partial \eta}{\partial \lambda} = \frac{I_{dc}}{4qB}\frac{m^2(m^2+16)\left[(3m^4+24m^2+8)-4(m^2+2)\lambda^2\right]}{\left[(3m^4+24m^2+8)+8(3m^2+2)\lambda+4(m^2+2)\lambda^2\right]^2} = 0. \qquad (4.4.24)$$

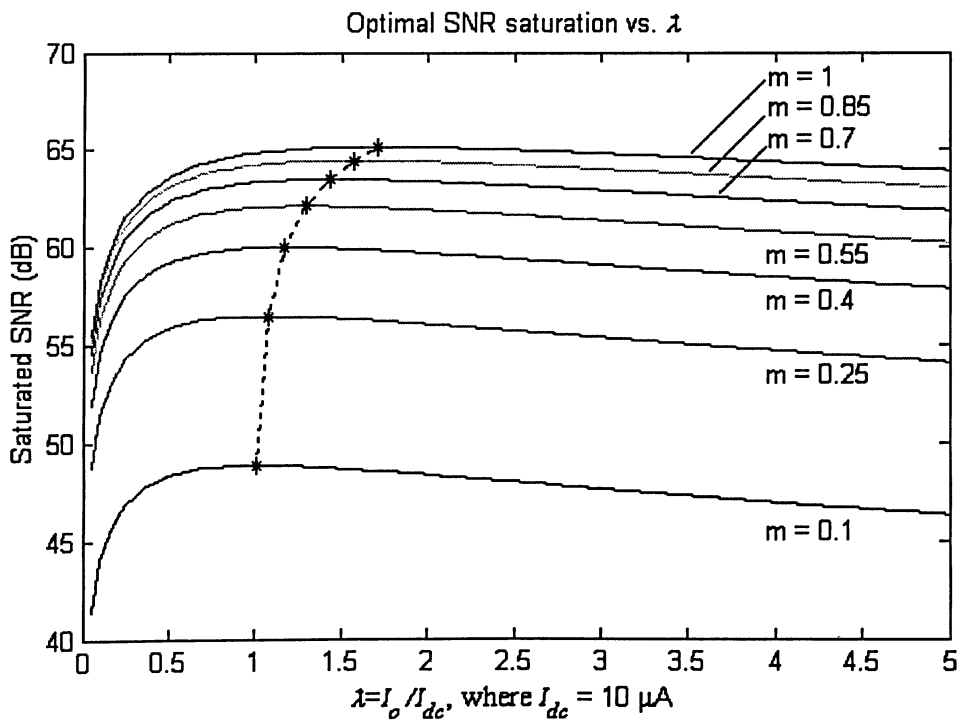

Figure 4.8 Saturated SNR against λ for Square Circuit

Hence,

$$\therefore \quad (3m^4 + 24m^2 + 8) - 4(m^2 + 2)\lambda^2 = 0,$$

$$\lambda = \sqrt{\frac{(3m^4 + 24m^2 + 8)}{4(m^2 + 2)}}. \tag{4.4.25}$$

For example, when m = 0.5, we get $\lambda = \sqrt{227}/12 \approx 1.2555$, i.e., when I_o = 1.2555 I_{dc}, we get the maximum SNR.

Figure 4.8 shows the trend of maximum value of λ when m varies from 0.1 to 1.

Through this optimal algorithm, we can design an appropriate value of λ, to get the best SNR, i.e., to reduce the influence of internal noise as much as possible.

4.4.3 Square-Root Circuit

This is another example of a second-order TL loop, it can be used to realise polynomials, rational functions and functions containing nth-order roots. The circuit is depicted in Figure 4.9.

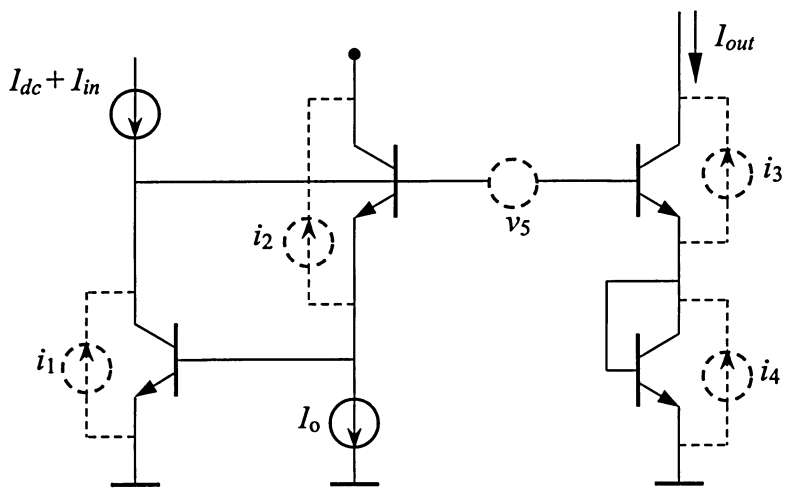

Figure 4.9 TL square-root circuit with noise sources

From the TL principle, considering the noise sources, we obtain:

$$(I_{dc} + I_{in} + i_1)(I_o + i_2) = (I_{out} + i_3)(I_{out} + i_4), \tag{4.4.26}$$

after rearranging this equation,

$$I_{out} = \sqrt{(I_{dc} + I_{in})I_o} + \frac{1}{2}\left(i_1\sqrt{\frac{I_o}{I_{dc} + I_{in}}} + i_2\sqrt{\frac{I_{dc} + I_{in}}{I_o}} - i_3 - i_4\right), \tag{4.4.27}$$

In this case, we found the first term of the right-hand-side is actually the summation of

$C(t)$ and $S(t)$. The second term is obviously the $T(t)$.

Using the previously elaborated noise analysis method, it is easy to get the time-dependent power spectral density function:

$$\begin{aligned} S_T(\omega,t) &= \frac{1}{2}\left[2qI_o + 2q(I_{dc}+I_{in}) + 2q\sqrt{(I_{dc}+I_{in})I_o} + 2q\sqrt{(I_{dc}+I_{in})I_o}\right] \\ &= q\left[I_o + I_{dc} + I_{in} + 2\sqrt{(I_{dc}+I_{in})I_o}\right] \\ &= q\left[I_o + I_{dc} + I_{in} + 2I_{out}\right] \end{aligned} \tag{4.4.28}$$

Because the average expectation of I_{out} is approximated equal to $\sqrt{I_o I_{dc}}(1-m^2/16)$ [12], the time-independent PSD is thus obtained:

$$\overline{S_T}(\omega) = q\left(I_o + I_{dc} + 2\sqrt{I_o I_{dc}}(1-m^2/16)\right), \tag{4.4.29}$$

where m is the modulation index of I_{in}.

4.5 Noise in Dynamic Translinear Circuits

In this section, the nonlinear noise characteristics of dynamic translinear ciruits, or in general, log-domain filters, will be discussed.

To large extent, the noise analysis method for DTL circuits is quite similar to those described in previous sections for STL circuits. However, because the existence of capacitance currents, which is frequency dependent, some more complicated analyses are necessary.

Some examples will be shown, such as class A and class AB translinear filters.

4.5.1 Noise Analysis Method

The TL loop principle, for example the equation (4.3.1), is suitable for both STL and DTL circuits. The only difference is the presence of the capacitance currents.

In order to find the DE representing the transfer function of a DTL circuit, the expressions for the capacitance currents have to be derived and substituted in the TL loop equation. Since the capacitance currents are related to collector currents incorporating

noise, the resulting capacitance noise expressions will include such noise sources and their derivatives. These derivatives of noise sources are additional elements, and are correlated to the noise sources from which they originate.

Thus the DE contains complicated noise terms, after manipulating the capacitance current expressions. Here, a first-order Taylor approximation of all noise sources and their derivatives can be used to simplify the expressions.

Since noise sources are correlated, they generate a colored frequency spectrum. Each autocorrelation function R_{Ti}, thus has to be computed collectively for an entire group of correlated noise sources.

Frequently, we can rewrite a group of correlated noise sources into one single expression of the form $i_i G_i$, where i_i represents a white noise source and G_i contains no noise sources. If this situation is accomplished, equations (4.3.9) and (4.3.10) can be used to calculate the noise frequency spectrum.

In addition, not all noise sources will be reflected at the output of the filter. So, we can only consider the noise terms that are situated in the expression of the output of the filter. To transform the noise terms to the output, those terms need to be multiplied by a certain frequency dependent transfer function. For example, if the filter transfer function is $H(\omega)$, the noise terms at input need to multiply $|H(\omega)|^2$.

4.5.2 Class-A Translinear Filter

This is a well-known DTL circuit, working as a first-order low-pass filter operating in class A. Its cut-off frequency can be tuned by the current I_o. It consists of a second-order TL loop, comprising $Q_1 - Q_4$, and a capacitor C, shown in Figure 4.10.

In the circuit, the noise voltages v_5 and v_6, are representing the base thermal noise of $Q_1 - Q_2$ and $Q_3 - Q_4$, respectively. They need to be transformed to the equivalent current noise sources. However, because the existence of the capacitor C in the TL loop, v_5 and v_6 cannot be combined to a single equivalent noise source. Instead, they are transformed to separate noise currents i_5 and i_6, which are in parallel with i_1 and i_4, respectively.

Therefore the equation of this TL loop comes into

$$(I_{dc}+I_{in}+i_1+i_5)(I_o+i_3)=(I_o+I_{cap}+i_2)(I_{dc}+I_{out}+i_4+i_6), \qquad (4.5.1)$$

where I_{cap} can be substituted by equation (3.2.16).

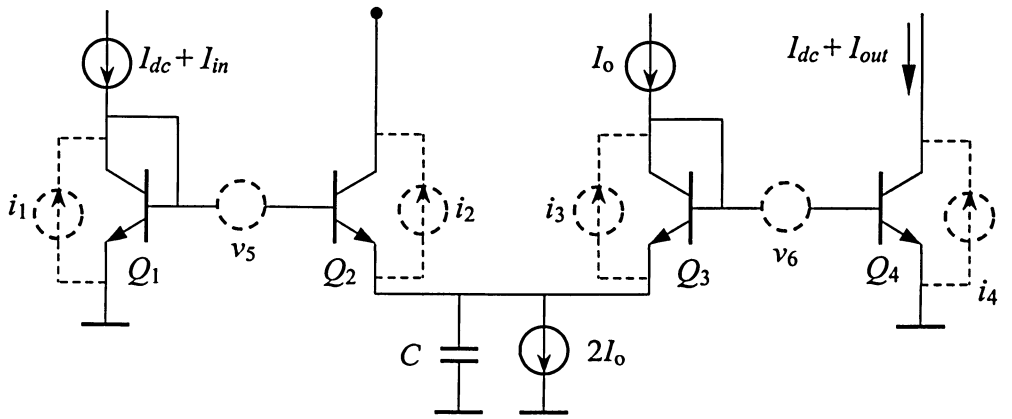

Figure 4.10 Class-A TL filter with noise sources

Using $i_{3,eq}=i_3\dfrac{I_{out}+I_{dc}}{I_o}$, which represents the equivalent noise source of i_3 at the output.

The above equation can be rewritten to

$$(I_{dc}+I_{in}+i_1+i_5)I_o=(I_o+I_{cap}+i_2)(I_{dc}+I_{out}+i_{3,eq}+i_4+i_6), \qquad (4.5.2)$$

where $I_{cap}=CU_T\dfrac{\partial(I_{dc}+I_{out}+i_{3,eq}+i_4+i_6)/\partial t}{(I_{dc}+I_{out}+i_{3,eq}+i_4+i_6)}$.

Through equation (4.5.2), we can get the input-output relation including first-order noise, ignoring the products of noise sources:

$$\frac{CU_T}{I_o}\left[(\dot{I}_{out}+\frac{d}{dt}(i_{3,eq}+i_4+i_6)\right]+I_{out}+i_{3,eq}+i_4+i_6=I_{in}+i_1+i_5-i_2\frac{I_{out}+I_{dc}}{I_o}, \qquad (4.5.3)$$

It is clear to find that i_1, i_2 and i_5 are associated with the input of the filter, while $i_{3,eq}$, i_4 and i_6 are located at the output.

In equation (4.5.3), we find two noise-signal intermodulation terms, i_2I_{out} assoicated with i_2, and i_3I_{out} associated with $i_{3,eq}$. Since $i_2 \ll I_{out}$ and $i_3 \ll I_{out}$, i_2 and i_3 are considered to be uncorrelated with I_{out}, thus the autocorrelation function $R(i_2I_{out}) = R(i_2)R(I_{out})$, and similarly, $R(i_3I_{out}) = R(i_3)R(I_{out})$. Therefore, the corresponding power spectral density can be obtained:

$$S(i_2 I_{out})(\omega,t) = \frac{1}{2\pi} S_{i_2}(\omega,t) * S_{I_{out}}(\omega,t)$$
$$= \frac{1}{2\pi} \int_{-\infty}^{\infty} S_{i_2}(y,t) S_{I_{out}}(\omega - y,t)\, dy \qquad (4.5.4)$$

where * stands for convolution.

Since i_2 is a white noise source, the above integral is easy to solve, and the PSD is given by:

$$S(i_2 I_{out})(\omega,t) = S_{i_2}(\omega,t) P_{I_{out}}, \qquad (4.5.5)$$

Similarly for i_3,

$$S(i_3 I_{out})(\omega,t) = S_{i_3}(\omega,t) P_{I_{out}}. \qquad (4.5.6)$$

where $P_{I_{out}}$ denotes the output power.

Thus the two noise spectra $S_{T_{in}}(\omega, t)$ and $S_{T_{out}}(\omega, t)$ can be obtained separately [29],

$$S_{T_{in}}(\omega,t) = 2q\left[\underbrace{(I_{dc} + I_{in})}_{i_1} + \underbrace{\frac{(I_o + I_{cap})(I_{dc} + I_{out})^2}{I_o^2}}_{i_2} + \underbrace{\frac{2R_B(I_{dc} + I_{in})^2}{U_T}}_{v_5}\right], \qquad (4.5.7a)$$

$$S_{T_{out}}(\omega,t) = 2q\left[\underbrace{\frac{(I_{dc} + I_{out})^2}{I_o}}_{i_3} + \underbrace{(I_{dc} + I_{out})}_{i_4} + \underbrace{\frac{2R_B(I_{dc} + I_{out})^2}{U_T}}_{v_6}\right], \qquad (4.5.7b)$$

where the horizontal brackets indicate the origin of the terms.

Then, we need to find out the time independent PSD. We use the enemble average of time dependent PSD. And we need to transform $S_{T_{in}}(\omega, t)$ to its output equivalent PSD, through $\overline{S_{T_{in}}}(\omega)|H(\omega)|^2$. Thus the whole average PSD $\overline{S_T}(\omega)$ is:

$$\overline{S_T}(\omega) = \tfrac{1}{T}\int_0^T \left[S_{T_{in}}(\omega,t)|H(\omega)|^2 + S_{T_{out}}(\omega,t)\right]dt$$
$$= 2q\left(I_{dc} + \frac{I_{dc}^2 + P_{I_{out}}}{I_o} + \frac{2R_B I_{dc}^2}{U_T}\right)\left(1 + |H(\omega)|^2\right) + \frac{4qR_B}{U_T}\left(P_{I_{out}} + P_{I_{in}}|H(\omega)|^2\right), \qquad (4.5.8)$$

where $P_{I_{in}} = \overline{I_{in}^2}$, $P_{I_{out}} = \overline{I_{out}^2}$, and $T = 2\pi/\omega_0$, the period of the input signal.

The transfer function of this filter can be obtained from the idealized TL loop equation followed by Fourier transform.

First, we have the idealized transfer function, derived from equation (4.5.1):

$$(I_{dc}+I_{in})I_{o}=(I_{o}+I_{cap})(I_{dc}+I_{out}), \tag{4.5.9}$$

Then, we can get the input-output relation. However, I_{cap} is an unknown, and need to be calculated specifically.

To better understand the calculation of I_{cap}, we refer to the Figure 4.11, which is the right part circuit of this filter. From the equation (3.2.14) to (3.2.16), we have,

$$I_{cap}=C\dot{V}_{cap}=C(\dot{V}_{BE4}-\dot{V}_{BE3})=CU_{T}\left(\frac{\dot{I}_{4}}{I_{4}}-\frac{\dot{I}_{3}}{I_{3}}\right)=CU_{T}\left(\frac{\dot{I}_{dc}+\dot{I}_{out}}{I_{dc}+I_{out}}-\frac{\dot{I}_{o}}{I_{o}}\right)$$

Because I_{o} and I_{dc} are all constants, their derivatives are zero, thus the I_{cap} turns to be:

$$I_{cap}=CU_{T}\frac{\dot{I}_{out}}{I_{dc}+I_{out}}. \tag{4.5.10}$$

Plugging (4.5.10) to (4.5.9), we get the input-output relation:

$$I_{in}I_{o}=I_{o}I_{out}+CU_{T}\dot{I}_{out}. \tag{4.5.11}$$

Applying Fourier transform, the transfer function of this filter is:

$$H(j\omega)=\frac{I_{o}}{I_{o}+j\omega CU_{T}}. \tag{4.5.12}$$

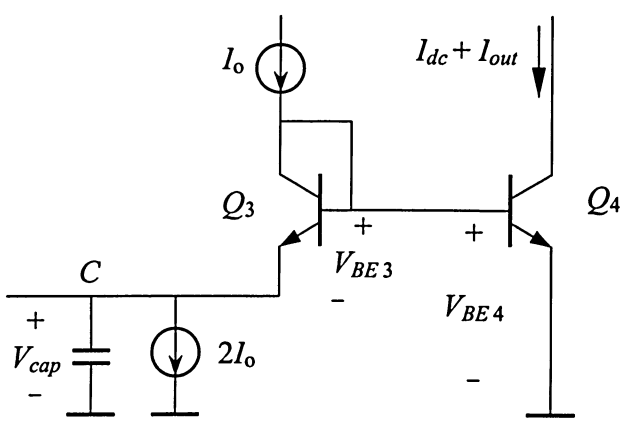

Figure 4.11 Part of Class-A TL filter

Suppose we have the input signal same as before, then we get the input power:

$$P_{I_{in}}=\overline{I_{in}^{2}}=\tfrac{1}{2}m^{2}I_{dc}^{2}. \tag{4.5.13}$$

Because this circuit is a low-pass filter, to simplify the calculation, suppose the power gain of this filter is unity, i.e., $P_{I_{in}}=P_{I_{out}}$.

The total output noise power is the integral of equation (4.5.8) over ω, at the bandwidth range $[-B, B]$, where $B = I_o / (2CU_T)$. Because only transfer function $H(j\omega)$ is function of ω, we can easily calculate the integral of $|H(j\omega)|^2$ first, and then multiply the other terms.

$$\int_{-\frac{2\pi I_o}{2CU_T}}^{\frac{2\pi I_o}{2CU_T}} |H(j\omega)|^2 d\omega = \int_{-\frac{2\pi I_o}{2CU_T}}^{\frac{2\pi I_o}{2CU_T}} \frac{I_o^2}{I_o^2 + (CU_T)^2 \omega^2} d\omega$$

$$= \frac{I_o^2}{(CU_T)^2} \int_{-\frac{2\pi I_o}{2CU_T}}^{\frac{2\pi I_o}{2CU_T}} \frac{1}{\left(\frac{I_o}{CU_T}\right)^2 + \omega^2} d\omega$$

$$= \frac{I_o^2}{(CU_T)^2} \cdot \frac{CU_T}{I_o} \arctan\left(\frac{CU_T}{I_o}\omega\right)\Bigg|_{-\frac{2\pi I_o}{2CU_T}}^{\frac{2\pi I_o}{2CU_T}}$$

$$= \frac{I_o}{CU_T} \cdot (\arctan\pi - \arctan(-\pi))$$

$$= 0$$

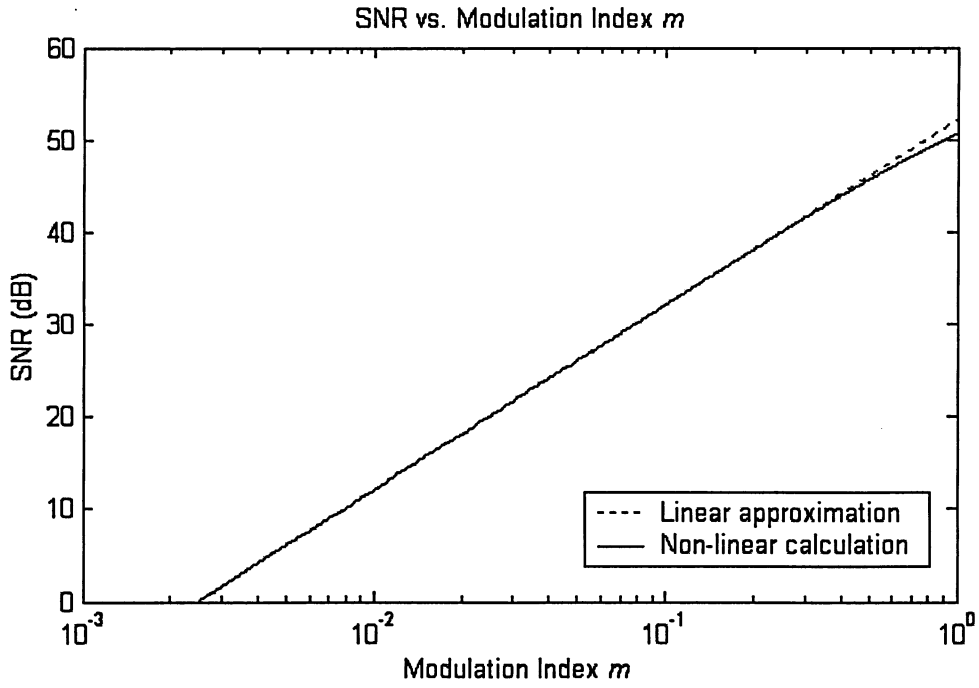

Figure 4.12 SNR ratio for a TL low-pass filter operated in Class-A

Thus, we can get the SNR of the class-A filter:

$$SNR = \frac{m^2 I_{dc}^2}{4q\frac{I_o}{CU_T}\left(I_{dc} + \frac{I_{dc}^2(1+\frac{1}{2}m^2)}{I_o} + \frac{2R_B I_{dc}^2}{U_T} + \frac{R_B m^2 I_{dc}^2}{U_T}\right)}. \quad (4.5.14)$$

Consider a sinusoidal input current within the passband of the filter, Figure 4.12 shows the SNR vs. modulation index m, where C = 10 pF, R_B = 600 Ω, I_{dc} = 5 μA, I_o = 1 μA, and B =1.92 MHz. Because this filter works in class-A, $m < 1$.

From this figure, we can find the signal-noise intermodulation influence is very small, since the linear approximation and non-linear calcualtion are so closed to each other. The difference is only equal to: 52.11 - 50.59 = 1.52 dB for $m = 1$.

Hence, for class-A TL filters, the noise floor in the absence of any signals can be used as a very good estimate of the noise.

4.5.3 Class-AB Translinear Filter

Since the current flowing through a transistor is always restricted to positive values, to process the signals of both negative and positive polarity, one popular option is to use push-pull stage, operated in class-AB.

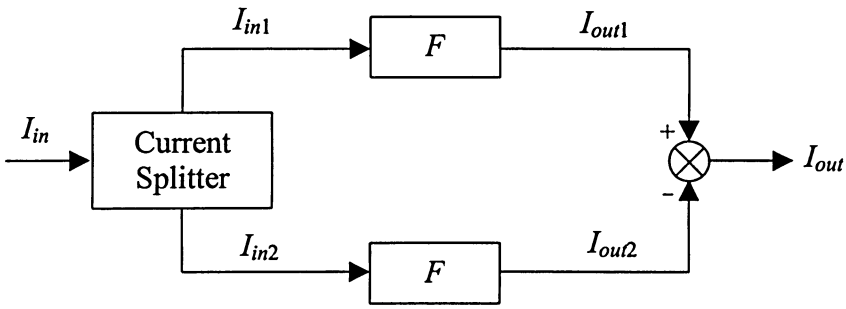

Figure 4.13 Principle of class-AB operation

That is to say that class-AB operation improves the DR of the companding system. To realise a class-AB first-order low-pass filter, firstly, we use a geometric mean current splitter, which will be explained later, to split the input current I_{in} to I_{in1} and I_{in2}. Then, apply them to the inputs of two class-A TL filters, described in the previous section. The dc bias current I_{dc} becomes useless and is omitted. The output currents of the two class-A filters are denoted by I_{out1} and I_{out2}. Again, the input signal is assumed to be sinusoidal,

see equation (4.4.7).

In class-AB operation, the input signal I_{in} firstly split into two strictly positive signals I_{in1} and I_{in2}. The difference equals the original signal I_{in}. Therefore, although I_{in1} and I_{in2} are strictly positive, the difference I_{in1} - I_{in2} can be negative values, thus is able to process bipolar signals. The two signals are processed separately, shown in Figure 4.13.

There are several current splitting strategies. A simple one is to set $I_{in1}= I_{in}$, when $I_{in} > 0$; otherwise, $I_{in1} = 0$. Similarly, when $I_{in} < 0$, $I_{in2} = -I_{in}$, otherwise, $I_{in2} = 0$. This one is known to work in class-B, it is simple but has an important disadvantage: the cross-over distortion.

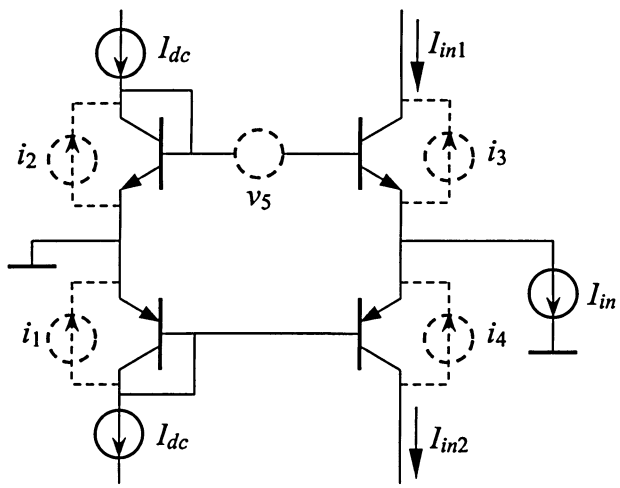

Figure 4.14 Geometric mean circuit splitter with noise sources

To avoid it, the transistors should never be completely turned off. In other words, it works in class-AB. A popular split strategy is as follows, using geometric mean function:

$$I_{in1,2} = \frac{1}{2}\left(\sqrt{4I_{dc}^2 + I_{in}^2} \pm I_{in}\right). \tag{4.5.15}$$

It can be implemented through the circuit shown in Figure 4.14. The output current of the splitter equals the difference of I_{in1} and I_{in2}, see Figure 4.15. Looking at the node at which the input current source is connected, it is clear that the output current is I_{in}, irrespective of the noise sources. This means that the splitter itself does not add any noise [12]. The noise sources present in the TL loop of this splitter only result in common-mode noise in I_{in1} and I_{in2}, which is irrelevant.

Using the equation (4.5.15) of geometric mean current splitter, the power $P_{I_{in1}}$ can be obtained:

$$P_{I_{in1}} = \overline{I_{in1}^2} = I_{dc}^2\left(1+\frac{1}{4}m^2\right), \tag{4.5.16}$$

where $I_{in1} = mI_{dc}\sin(\omega_0 t + \phi)$.

In this system, the average of output current is same as the average of input current, i.e., $\overline{I_{in1}} = \overline{I_{out1}}$. However, the exact expression can not be calculated, as the input is a sine wave, see equation (4.4.7).

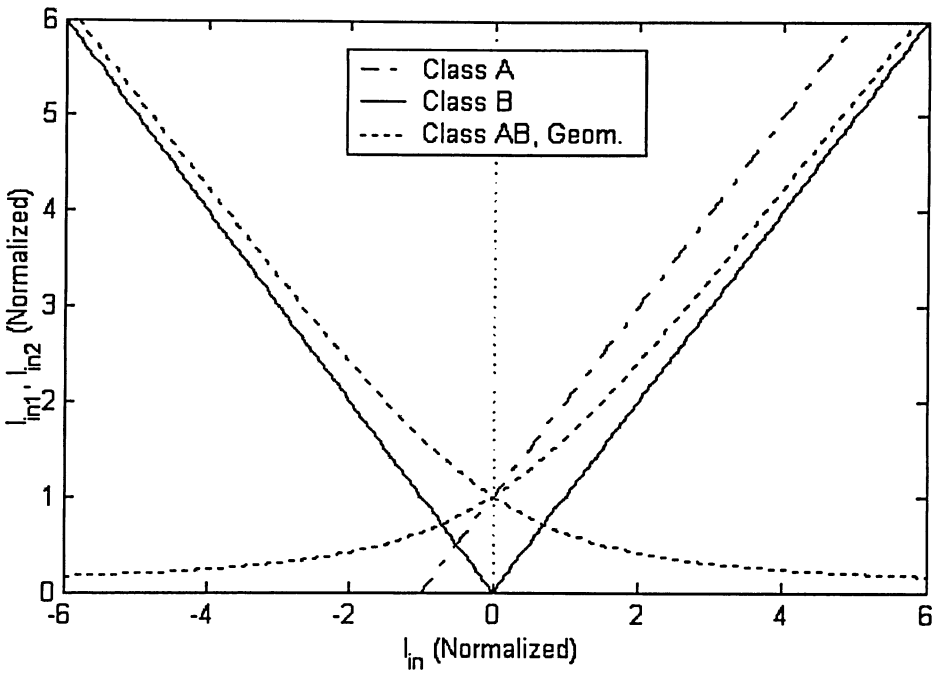

Figure 4.15 The currents resulting from different splitters

But, for noise purpose, we can still get the approximated value by:

$$\overline{I_{in1}} = \overline{I_{out1}} = \begin{cases} I_{dc}, & m << 1 \\ \dfrac{m}{2}I_{dc}, & m >> 1 \end{cases} \tag{4.5.17}$$

Figure 4.16 illustrates the relation between the exact value and approximation of the dc output current level.

In class AB, the bias dc current I_{dc} is obsolete and therefore omitted. Thus, the expressions of two two noise spectra $S_{T_{in}}(\omega, t)$ and $S_{T_{out}}(\omega, t)$, shown in equation (4.5.7a) and (4.5.7b), is modified to:

$$S_{T_{in}}(\omega,t) = 2q\left[I_{in} + \frac{(I_o + I_{cap})I_{out}^2}{I_o^2} + \frac{2R_B I_{in}^2}{U_T}\right], \tag{4.5.18a}$$

$$S_{T_{out}}(\omega,t) = 2q\left[\frac{I_{out}^2}{I_o} + I_{out} + \frac{2R_B I_{out}^2}{U_T}\right], \tag{4.5.18b}$$

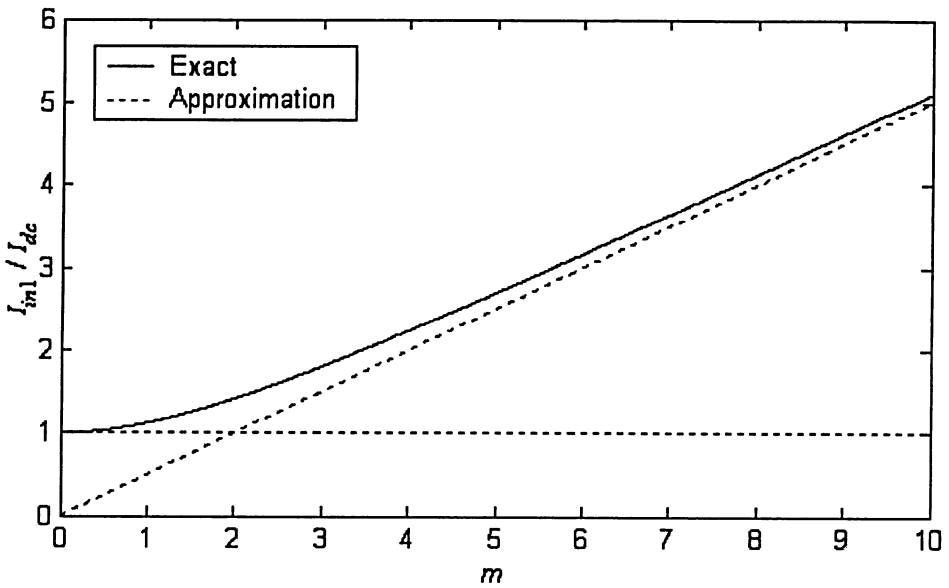

Figure 4.16 The dc output level of a geometric mean splitter

Similarly, the total time-independent output noise PSD is obtained.

Assuming the influence of R_B is negligible, the computation of the average sepctrum of PSD becomes:

$$\begin{aligned}\overline{S_{T1}}(\omega) &= \tfrac{1}{T}\int_0^T \left[S_{T_{in1}}(\omega,t)\left|H(\omega)\right|^2 + S_{T_{out1}}(\omega,t)\right]dt \\ &= 2q\left(\overline{I_{out1}} + \frac{P_{I_{out1}}}{I_o} + \frac{2R_B P_{I_{out1}}}{U_T}\right)\left(1 + \left|H(\omega)\right|^2\right)\end{aligned} \tag{4.5.19}$$

where $P_{I_{out1}}$ is the power of I_{out1}, i.e., $P_{I_{out1}} = \overline{I_{out1}^2}$, and $H(\omega)$ is the transfer function.

Using integration of the equation (4.5.19) over ω, then times 2 for two class-A filters, and finally multiply the noise bandwidth $2B = I_o / (CU_T)$, we thus obtain the time-independent noise power. So, the SNR is given by:

$$SNR = \frac{CU_T m^2 I_{dc}^2}{8qI_{dc}\left[\frac{m}{2}I_o + I_{dc}\left(1+\frac{1}{4}m^2\right)+\frac{2R_B I_{dc} I_o}{U_T}\left(1+\frac{1}{4}m^2\right)\right]}$$
$$= \frac{CU_T I_{dc}}{2q\left[\frac{2I_o}{m} + I_{dc}\left(1+\frac{2R_B I_o}{U_T}\right)\left(1+\frac{4}{m^2}\right)\right]} \qquad (4.5.20)$$

The SNR is a function of the modulation index m of the input signal. Figure 4.17 is the simulation result, where the parameters are: $I_{dc} = aI_o$, where a = [0.1, 1, 10], C = 10 pF, R_B = 600 Ω, I_o = 1 μA, and U_T = 26 mV. The x-axis variable, $m*a$, represents the amplitude of I_{in}, normalised to I_o. When $m*a$ is at low values, the SNR increases linearly at 20 dB per decade, and lower value of I_{dc} leads to higher SNR level. Eventually the SNR saturates at 58.9 dB.

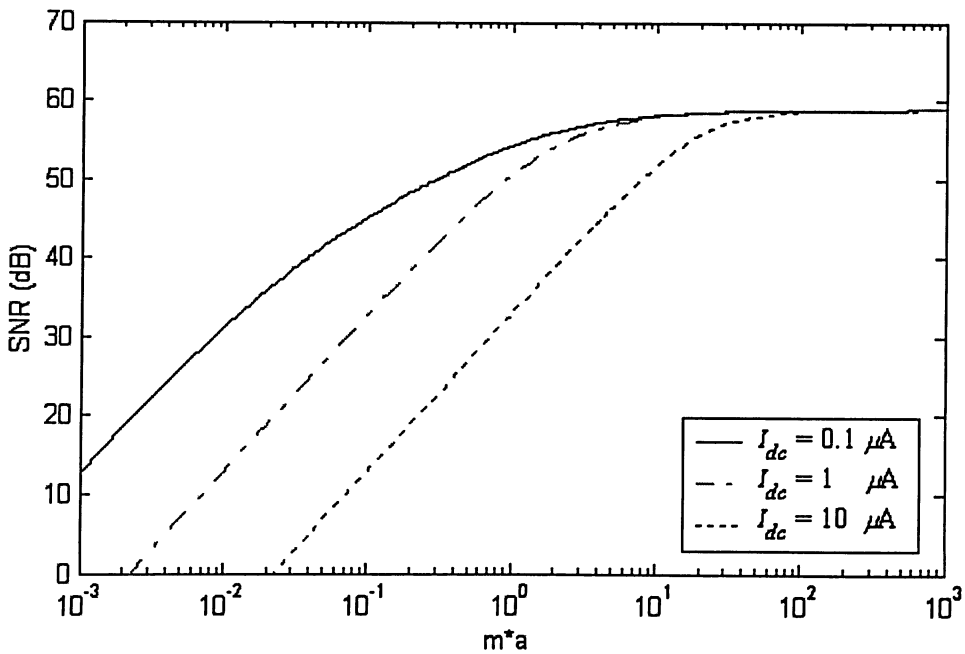

Figure 4.17 SNR of a class-AB translinear circuit

The maximal SNR is

$$\lim_{m\to\infty} SNR = \frac{CU_T}{2q\left(1+\frac{2R_B I_o}{U_T}\right)}. \qquad (4.5.21)$$

In lower current level, the expression of limitation of SNR approximately equals:

$$\lim_{m\to\infty} SNR = \frac{CU_T}{2q}, \tag{4.5.22}$$

since the influence of thermal noise is negligible. For example, in the above setting, $\frac{2R_B I_o}{U_T} = 0.0462$, which is much smaller than 1.

While at high current level, the thermal noise becomes dominant, i.e., $\frac{2R_B I_o}{U_T} >> 1$, then the saturation level of SNR is given by:

$$\lim_{m\to\infty} SNR = \frac{CU_T^2}{4qR_B I_o}. \tag{4.5.23}$$

Chapter 5

An Alternative Noise Analysis Method

In this chapter, an alternative noise analysis method is discussed. In previous section, all the noise sources are combined and/or moved to output port, before computing the noise power spectral density and signal-to-noise ratio. On the other hand, this method is to analyze the influence of all noise sources directly and individually, without any need to combining or moving them. Because, in principle, the noise sources are supposed to be uncorrelated to each other, this way will not affect the analysis result.

From the previous chapter, we know that the total equivalent noise current at the collector terminal of a transistor is the summation of collector current shot noise and base resistance thermal noise, ignoring the other two noise sources, base shot noise and flicker noise, which are relatively small and negligible. Actually, in most cases, the circuit is working on a low level dc current, which means that the base resistance thermal noise has much smaller influence than collector shot noise, thus also can be ignored.

In the following analysis, for simplicity, we will just consider the collector shot noise source.

We will still use $\overline{(\cdot)}$ to represent the average value over time.

5.1 Noninverting Integrator

This is a very popular dynamic translinear circuit, which used in a variety of filters, such as Seevink's class AB TL filter [6], low-pass log-domain biquad filter [17], etc.

As a part of a filter, I_q is typically connected with another TL loop to form a higher-order filter. When it is a dc current, it provides damping and implements local negative feedback [17].
The TL loop equation can be derived from the basic TL principle,

$$(I_{in}+i_1)(I_o+i_2)=(I_{cap}+i_3)(I_{out}+i_4). \qquad (5.1.1)$$

The corresponding lossless TL equation is then obtained:

$$I_{in}I_o=I_{cap}I_{out}. \qquad (5.1.2)$$

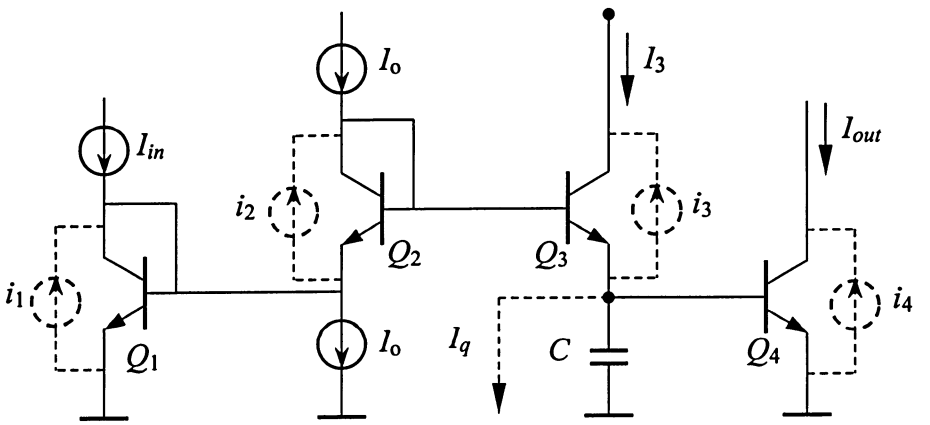

Figure 5.1 Noninverting integrator with noise sources

where $I_{cap} = CU_T \dot{I}_{out}/I_{out}$, plugging this condition to the above equation (5.1.2), we get the DE and then transfer-function in frequency domain by applying Fouier transform.

$$I_{in}I_o = CU_T \frac{\dot{I}_{out}}{I_{out}} I_{out} = CU_T \dot{I}_{out}$$

$$\therefore H(s) = \frac{I_{out}(s)}{I_{in}(s)} = \frac{I_o}{sCU_T} \tag{5.1.3}$$

Next, to transform the noise sources i_1, i_2, and i_3 to the output, we also need to know the transfer function at I_{out} over I_o and I_3, respectively.

$$H_{Io}(s) = \frac{I_{out}(s)}{I_o(s)} = \frac{I_{out}(s)}{I_{in}(s)} \cdot \frac{I_{in}(s)}{I_o(s)} = \left(\frac{I_{in}}{I_o}\right)\frac{I_o}{sCU_T} \tag{5.1.4}$$

$$H_{I3}(s) = \frac{I_{out}(s)}{I_3(s)} = \frac{I_{out}}{I_o}\frac{I_{out}}{I_{in}} = \left(\frac{I_{out}}{I_o}\right)\frac{I_o}{sCU_T} \tag{5.1.5}$$

Now ,we introduce two definitions: noise scaling factor k_n for noise n and intrinsic noise transfer function $N(s)$. This is done by removing I_{in} and I_o in (5.1.2), and replacing them with a noise source n and the noise scaling factor k_n. We get:

$$k_n n = sCU_T I_{out}. \tag{5.1.6}$$

Then,
$$\frac{I_{out}}{n} = \frac{k_n}{sCU_T} = k_n N(s). \tag{5.1.7}$$

By comparing equation (5.1.4), (5.1.5) and (5.1.7), we find the scaling factor and intrinsic noise transfer function to be:

$$k_n = I_o,$$
$$N(s) = \frac{1}{sCU_T}. \tag{5.1.8}$$

The power spectral density of each noise sources at the output can be obtained:

$$S_{i_1}(\omega) = \overline{i_1^2}|H(\omega)|^2 = 2q\overline{I_{in}}\left|\frac{I_o}{j\omega CU_T}\right|^2, \tag{5.1.9}$$

$$S_{i_2}(\omega) = \overline{i_2^2}|H_{Io}(\omega)|^2 = 2qI_o\left(\frac{\overline{I_{in}^2}}{I_o^2}\right)\left|\frac{I_o}{j\omega CU_T}\right|^2, \tag{5.1.10}$$

$$S_{i_3}(\omega) = \overline{i_3^2}|H_{I3}(\omega)|^2 = 2q\overline{I_3}\left(\frac{\overline{I_{out}^2}}{I_o^2}\right)\left|\frac{I_o}{j\omega CU_T}\right|^2, \tag{5.1.11}$$

$$S_{i_4}(\omega) = \overline{i_4^2} = 2q\overline{I_{out}}. \tag{5.1.12}$$

Because all the noise sources are independent to each other, the total output noise PSD is:

$$S_{total}(\omega) = S_{i_1}(\omega) + S_{i_2}(\omega) + S_{i_3}(\omega) + S_{i_4}(\omega). \tag{5.1.13}$$

In the above PSD equations, all the PSDs are in the form of time-independent ensembles. However, the currents are originally time-dependent, e.g., I_{in} is actually $I_{in}(\omega,t)$. Thus, before we calculate each PSD term, we need to compute the time-independent current expressions. The method is to acquire the time average ensemble according to one signal period T.

In time-domain, the transfer function becomes:

$$I_{out} = \frac{I_o}{CU_T}\int I_{in}dt. \tag{5.1.14}$$

Suppose we have the input signal:

$$I_{in} = I_{dc} + mI_{dc}\sin(\omega_0 t + \phi), \tag{5.1.15}$$

where m is the modulation index, ω_0 is the signal frequency, and ϕ is a uniformly distributed stochastic variable, representing the arbitrary choice of the origin of the time axis.

So, the corresponding average current and square value are:

$$\overline{I_{in}} = I_{dc}, \tag{5.1.16}$$

$$\overline{I_{in}^2} = \frac{1}{T}\int_0^T I_{dc}^2 dt = I_{dc}^2\left(1 + \frac{1}{2}m^2\right), \tag{5.1.17}$$

Plugging equation (5.1.15) into (5.1.14), we get:

$$
\begin{aligned}
I_{out}(t) &= \frac{I_o}{CU_T}\int [I_{dc} + mI_{dc}\sin(\omega_0 t + \phi)]dt \\
&= \frac{I_o I_{dc}}{CU_T}\left(t - \frac{m}{\omega_0}\cos(\omega_0 t + \phi)\right)
\end{aligned}
\tag{5.1.18}
$$

Thus, we can obtain the average of output current by:

$$
\overline{I_{out}} = \frac{1}{T}\int_0^T I_{out}(t)dt = \frac{I_o I_{dc}}{CU_T}\frac{1}{T}\int_0^T t - \frac{m}{\omega_0}\cos(\omega_0 t + \phi)dt = \frac{I_o I_{dc}}{CU_T}. \tag{5.1.19}
$$

The square of the output current is given by:

$$
\begin{aligned}
\overline{I_{out}^2} &= \frac{1}{T}\int_0^T I_{out}^2(t)dt \\
&= \left(\frac{I_o I_{dc}}{CU_T}\right)^2 \frac{1}{T}\int_0^T (t - \frac{m}{\omega_0}\cos(\omega_0 t + \phi))^2 dt\,, \\
&= \left(\frac{I_o I_{dc}}{CU_T}\right)^2 \left(\frac{4\pi^2}{3\omega_0^2} + \frac{m^2}{2\pi\omega}\right)
\end{aligned}
\tag{5.1.20}
$$

It is a little bit tricky to get the average value of current I_3. We know that

$$
I_3 = CU_T\frac{\dot{I}_{out}}{I_{out}}, \tag{5.1.21}
$$

hence,

$$
\begin{aligned}
\overline{I_3} &= \frac{1}{T}\int_0^T CU_T\frac{\dot{I}_{out}}{I_{out}}dt = CU_T\frac{1}{T}\int_0^T \frac{1}{I_{out}}dI_{out} \\
&= CU_T\frac{1}{T}\ln(I_{out})\Big|_0^T = \frac{CU_T}{T}\ln\left(\frac{I_{out}(T)}{I_{out}(0)}\right) \\
&= \frac{CU_T\omega_0}{2\pi}\ln\left(\frac{m-2\pi}{m}\right)
\end{aligned}
\tag{5.1.22}
$$

Now, we can get the noise power spectral density expression by plugging equations (5.1.16) – (5.1.22) into (5.1.13).

Note that the above circuit is not complete, because capacitor C can not be discharged. And this can be solved by add discharging elements, which will be discussed in next section.

5.2 Inverting Integrator

In this circuit, we add two transistors to discharge the capacitor, shown in Figure 4.11. The current flowing through Q_{x2} is to discharge the capacitor C.

Using the same TL principle, the lossless TL equation of the inverting integrator is obtained. Actually, we just add redundant terms on both sides of equation (5.1.2) [17].

$$(I_{in}+I_{out})I_o=(I_o-I_{cap})I_{out}. \tag{5.2.1}$$

Thus, the transfer function becomes:

$$H(s)=\frac{I_{out}(s)}{I_{in}(s)}=-\frac{I_o}{sCU_T} \tag{5.2.2}$$

Then, the transfer function from I_o to the output are:

$$H_{Io}(s)=\frac{I_{out}(s)}{I_o(s)}=-\frac{I_{in}}{I_o}\frac{I_o}{sCU_T} \tag{5.2.3}$$

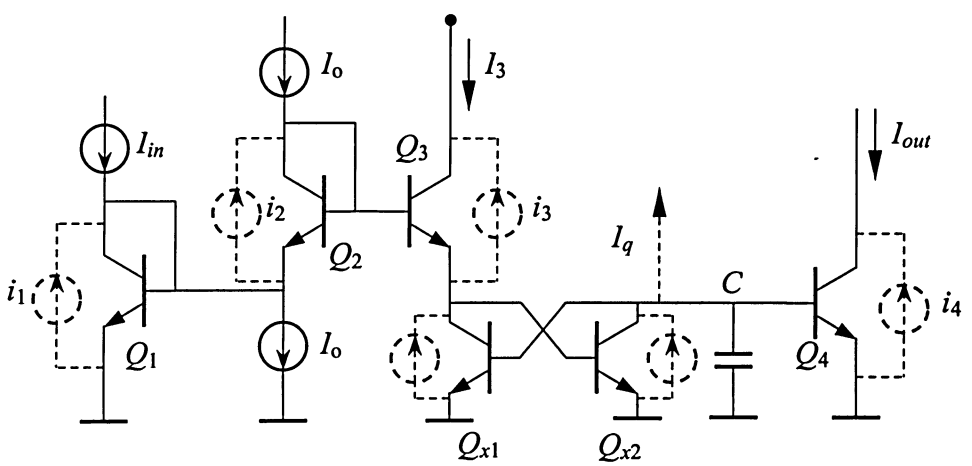

Figure 5.2 Inverting integrator with noise sources

The current flowing through Q_{x2} is the actual inverted collector current I_3, so the transfer function is:

$$H_{Ix2}(s)=\frac{I_{out}(s)}{I_{x2}(s)}=\frac{-I_{out}}{I_o}\frac{-I_o}{sCU_T}=\frac{I_{out}}{I_o}\frac{I_o}{sCU_T} \tag{5.2.4}$$

The current I_3 flows through both Q_3 and Q_{x1}, and is actually the same as I_{out}, since the bases of Q_{x1} and Q_4 are connected together. Hence the transfer function is:

$$H_3(s)=\frac{I_{out}(s)}{I_3(s)}=\frac{I_{in}}{I_{out}}\frac{-I_o}{sCU_T} \tag{5.2.5}$$

Then, we can calculate the expressions for these noise PSDs to the output separately, since they are uncorrelated to each other.

$$S_{i_1}(\omega) = \overline{i_1^2}\left|H(\omega)\right|^2 = 2q\overline{I_{in}}\left|\frac{-I_o}{j\omega CU_T}\right|^2, \tag{5.2.6}$$

$$S_{i_2}(\omega) = \overline{i_2^2}\left|H_{Io}(\omega)\right|^2 = 2qI_o\left(\frac{I_{in}}{I_o}\right)^2\left|\frac{-I_o}{j\omega CU_T}\right|^2, \tag{5.2.7}$$

$$S_{i_3}(\omega) = S_{i_{x1}}(\omega) = \overline{i_3^2}\left|H_{Io}(\omega)\right|^2 = 2q\overline{I_{out}}\left(\frac{I_{in}}{I_{out}}\right)^2\left|\frac{-I_o}{j\omega CU_T}\right|^2, \tag{5.2.8}$$

$$S_{i_{x2}}(\omega) = \overline{i_{x2}^2}\left|H_{Io}(\omega)\right|^2 = 2q\overline{I_3}\left(\frac{I_{out}}{I_o}\right)^2\left|\frac{I_o}{j\omega CU_T}\right|^2, \tag{5.2.9}$$

So, the total noise power spectral density is:

$$S_{total}(\omega) = S_{i_1}(\omega) + S_{i_2}(\omega) + S_{i_{x2}}(\omega) + 2S_{i_3}(\omega) + S_{i_4}(\omega). \tag{5.2.10}$$

The factor 2 accounts for the fact that I_3 flows through both Q_3 and Q_{x1}.

Similar to the noninverting integrator discussed in previous section, all the PSD terms in equation (5.2.10) are time-independent ensembles, therefore need to be computed from original time-dependent forms. Please refer to equations (5.1.14) – (5.1.22) for details.

5.3 Second-Order Low-Pass Translinear Biquad

The schematic of a second-order low-pass translinear biquad is depicted in Figure 5.3. It comprises two integrators.

In this circuit, for calculation purpose, we add an fictious transistor I_{v1}, as an intermediate output transistor. This circuit was thoroughly analyzed in [17]. Denote $H_1(s)$ as the transfer function from input to the fictious transistor I_{v1}, while $H_2(s)$ as from input to output. Therefore we obtained the following transfer functions:

$$H_1(s) = \frac{I_{v1}}{I_{in}} = \frac{\dfrac{I_{o1}(sCU_T + I_d)}{(CU_T)^2}}{s^2 + \dfrac{I_d}{CU_T}s + \dfrac{I_{o2}I_{o3}}{(CU_T)^2}}, \tag{5.3.1}$$

$$H_2(s) = \frac{I_{out}}{I_{in}} = \frac{\dfrac{I_{o2}I_{o3}}{(CU_T)^2}}{s^2 + \dfrac{I_d}{CU_T}s + \dfrac{I_{o2}I_{o3}}{(CU_T)^2}}, \tag{5.3.2}$$

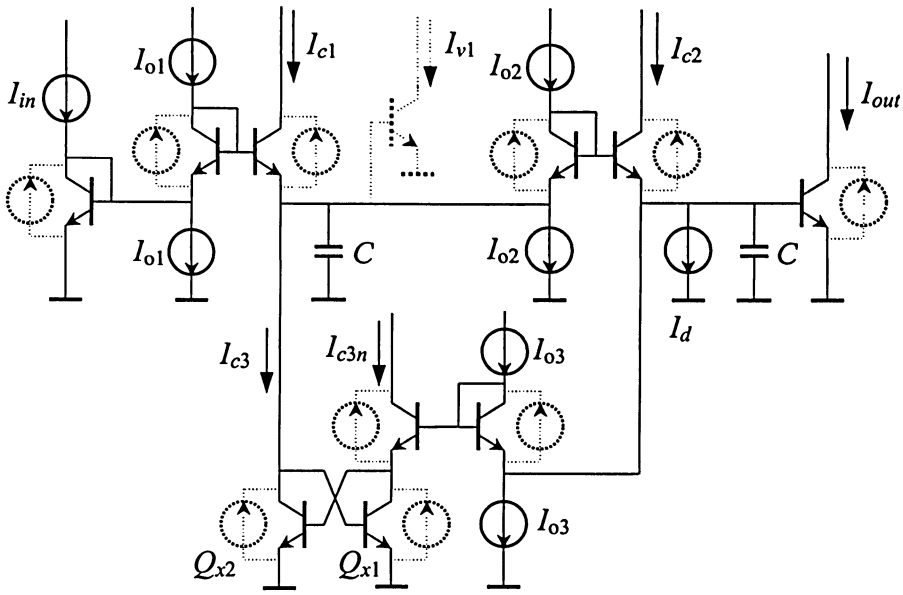

Figure 5.3 Second-order low-pass TL biquad with noise sources

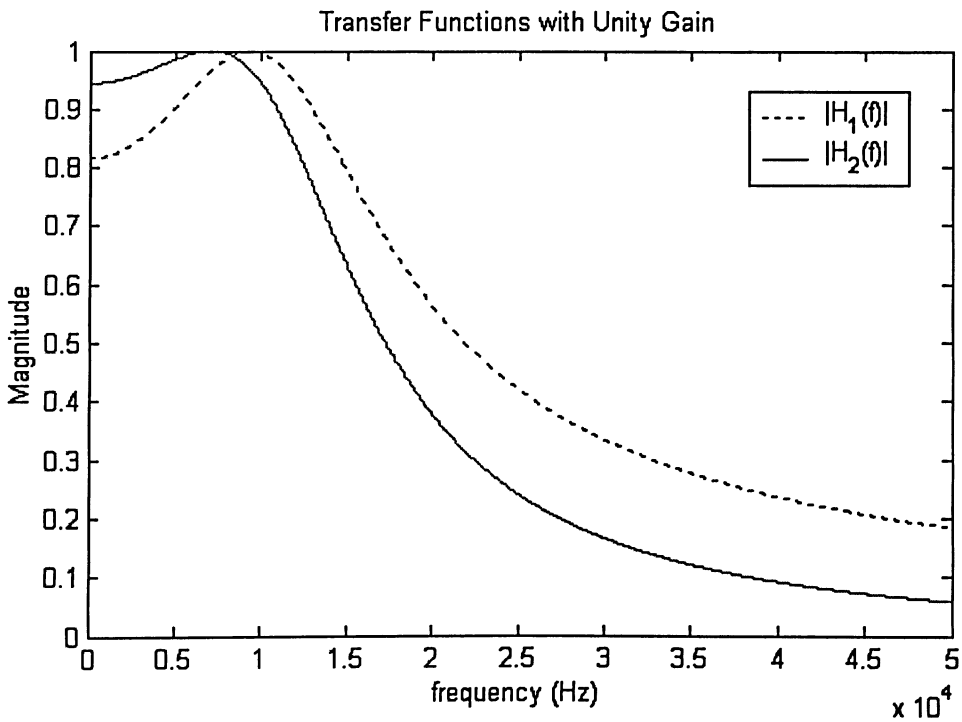

Figure 5.4 Signal transfer function

Similarly, removing the currents I_{in} and I_{o1}, and injecting noise currents into each integrating node one by one, we can derive the intrinsic noise transfer functions:

$$N_1(s) = \frac{\frac{I_{o2}}{(CU_T)^2}}{s^2 + \frac{I_d}{CU_T}s + \frac{I_{o2}I_{o3}}{(CU_T)^2}}, \tag{5.3.3}$$

$$N_2(s) = \frac{\frac{1}{CU_T}s}{s^2 + \frac{I_d}{CU_T}s + \frac{I_{o2}I_{o3}}{(CU_T)^2}}, \tag{5.3.4}$$

where $N_1(s)$ represents the transfer function from I_{v1} to output, while $N_2(s)$ represents the transfer function from I_{c2} to output.

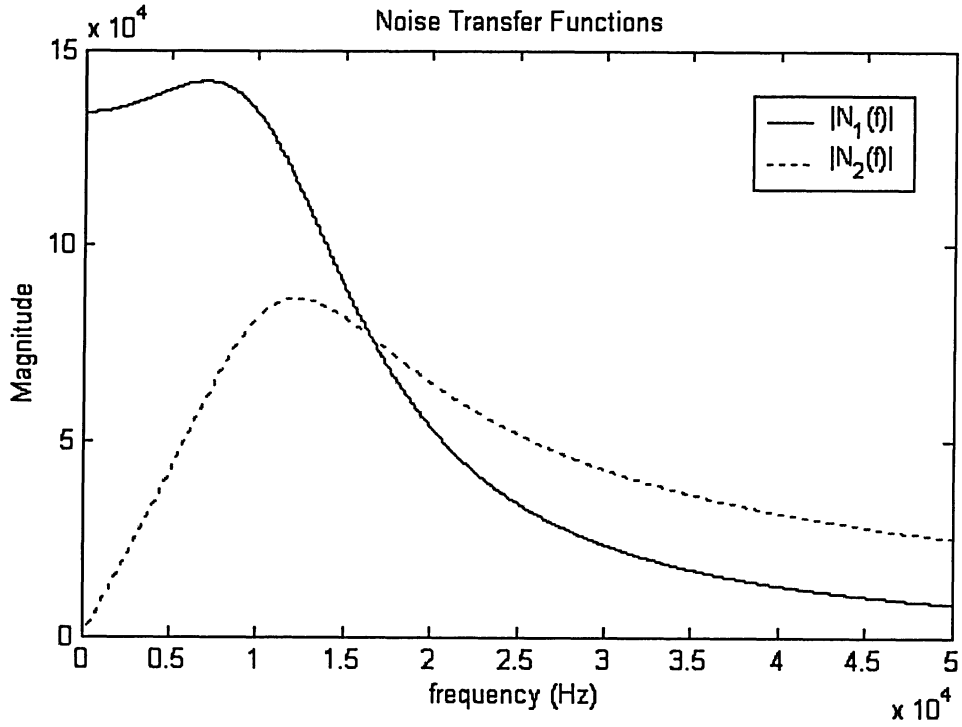

Figure 5.5 Intrinsic noise transfer function

Figure 5.4 and 5.5 show the simulations of signal transfer functions and intrinsic noise transfer function, respectively.

The elements of the circuit used in the simulation are:
$I_{o1} = 7.048\ \mu A$, $I_{o2} = 13.40\ \mu A$, $I_{o3} = 7.465\mu A$, $I_d = 11.58\ \mu A$, and $C = 4.970$ nF .

For a sinusoidal input signal $I_{in} = I_{dc} + A\sin(2\pi f_s t)$, the signals at intemediate and output ports are simply scaled and phase-shifted, since the system has a linear-time-invariant transfer function. For writing convenience, denote $I_{v2}(t)= I_{out}(t)$, then:

$$I_{vi}(t) = I_{dc}|H_i(0)| + A|H_i(f_s)|\sin(2\pi f_s t + \phi_i(f_s)), \tag{5.3.5}$$

where $\phi_i(f) = \arctan\left(\frac{\mathrm{Im}(H_i(f))}{\mathrm{Re}(H_i(f))}\right)$. (5.3.6)

Applying the translinear principle to the sub-loops of the biquad, we can get the other lossless collect currents:

$$I_{c1}(t) = \frac{I_{in}(t)}{I_{v1}(t)} I_{o1}, \tag{5.3.7}$$

$$I_{c2}(t) = \frac{I_{v1}(t)}{I_{out}(t)} I_{o2}, \tag{5.3.8}$$

$$I_{c1}(t) = \frac{I_{out}(t)}{I_{v1}(t)} I_{o3}, \tag{5.3.9}$$

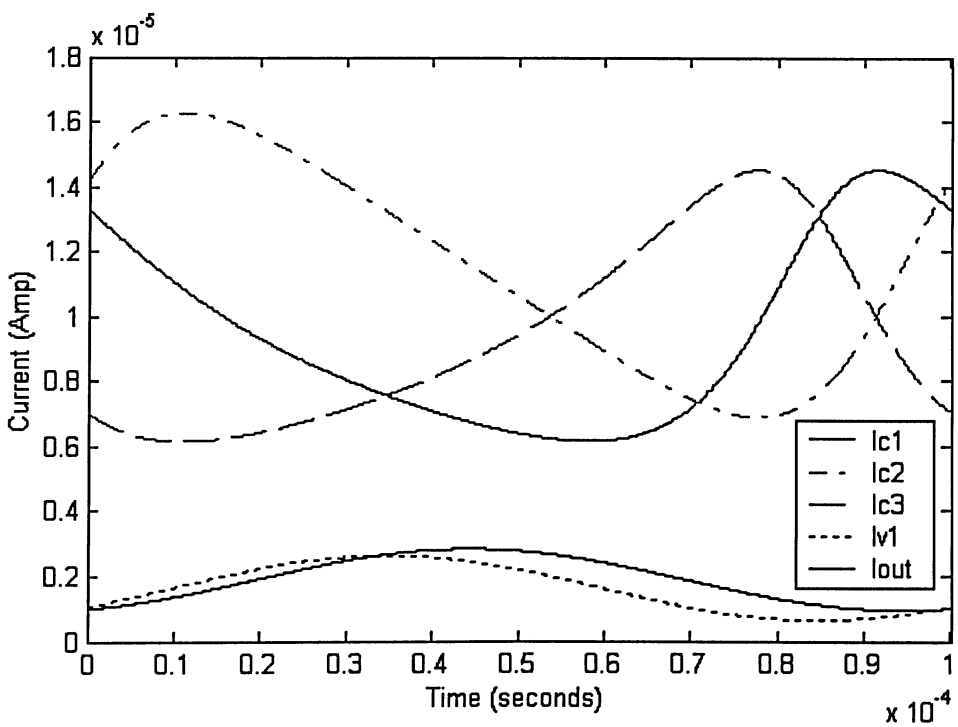

Figure 5.6 Log-domain biquad filter current waveforms

Figure 5.6 shows the waveforms of these currents in one period. Assume the signal frequency is 10 KHz, $I_{dc} = 2\ \mu$A, and $A = 1\ \mu$A.

Now we can calculate the power spectral density of each noise source, at the output. Start from the TL sub-loop including the input,

$$S_{in}(\omega) = 2q\overline{I_{in}}|H_2(\omega)|^2, \tag{5.3.10}$$

$$S_{I_{o1}}(\omega) = 2qI_{o1}\left(\frac{I_{in}}{I_{o1}}\right)^2 \left(I_{o1}|N_1(\omega)|\right)^2, \tag{5.3.11}$$

$$S_{I_{c1}}(\omega) = 2q\overline{I_{c1}}\left(\frac{I_{v1}}{I_{o1}}\right)^2 \left(I_{o1}|N_1(\omega)|\right)^2. \tag{5.3.12}$$

Then the sub-loop including the output,

$$S_{I_{o2}}(\omega) = 2qI_{o2}\left(\frac{I_{v1}}{I_{o2}}\right)^2 \left(I_{o2}|N_2(\omega)|\right)^2, \tag{5.3.13}$$

$$S_{I_{c2}}(\omega) = 2q\overline{I_{c2}}\left(\frac{I_{out}}{I_{o2}}\right)^2 \left(I_{o2}|N_2(\omega)|\right)^2, \tag{5.3.14}$$

$$S_{out}(\omega) = 2q\overline{I_{out}}. \tag{5.3.15}$$

Finally, the sub-loop located at the bottom part of the circuit,

$$S_{I_{o3}}(\omega) = 2qI_{o3}\left(\frac{I_{out}}{I_{o3}}\right)^2 \left(I_{o3}|N_1(\omega)|\right)^2, \tag{5.3.16}$$

$$S_{I_{c3}}(\omega) = 2q\overline{I_{c3}}\left(\frac{I_{v1}}{I_{o3}}\right)^2 \left(I_{o3}|N_1(\omega)|\right)^2, \tag{5.3.17}$$

$$S_{I_{c3n}}(\omega) = 2q\overline{I_{v1}}\left(\frac{I_{out}}{I_{v1}}\right)^2 \left(I_{o3}|N_1(\omega)|\right)^2, \tag{5.3.18}$$

where the time-average stands for $\overline{(\cdot)} = \frac{1}{T}\int_0^T (\cdot)dt$. As for the terms containing square of I_{in}, I_{out}, and I_{v1}, because they are functions of time t, we need to use $(\cdot)^2 = \frac{1}{T}\int_0^T (\cdot)^2 dt$ to acquire the time-independent expressions before calculating the PSDs over ω.

Therefore, we get the total output noise PSD by combining equations (5.3.10) – (5.3.18) :

$$S_{total}(\omega) = S_{in}(\omega) + \sum_i S_{I_{oi}}(\omega) + \sum_i S_{I_{ci}}(\omega) + 2S_{I_{c3n}}(\omega) + S_{out}(\omega), \tag{5.3.19}$$

where again, the factor 2 comes from the fact that I_{c3n} flows through both Q_{Ic3n} and Q_{x1}. Figure (5.7) shows the simulation of root noise spectral density at the output, with various input dc current levels.

The root total power spectral density $\sqrt{S_{total}(\omega)}$ was simulated in SpectreRF in [17], and they are very well matched with the method described in this section.

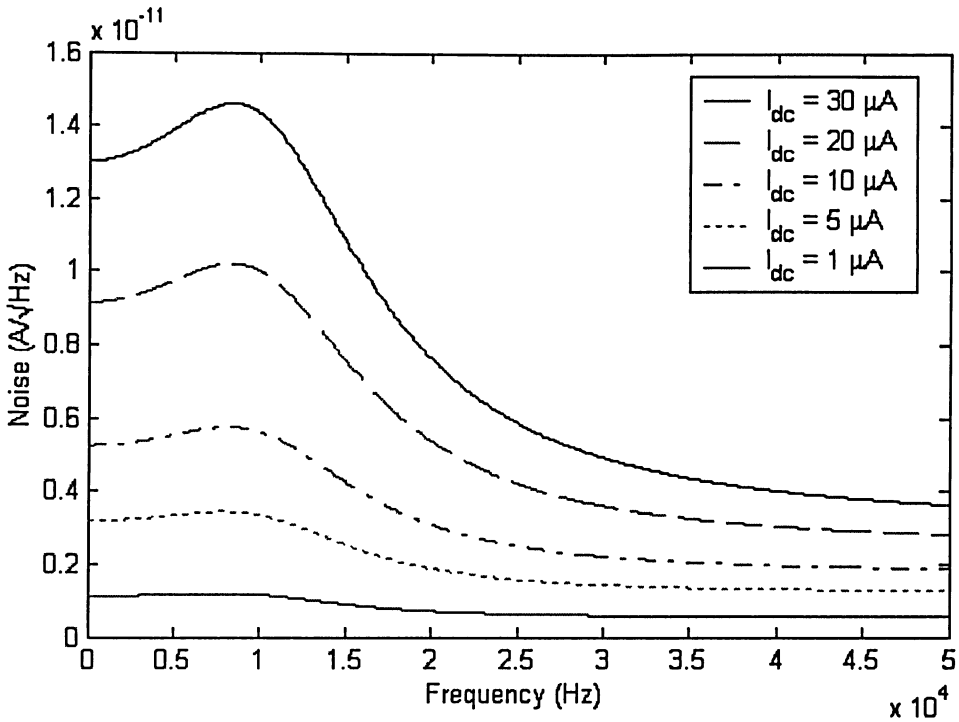

Figure 5.7 Output noise with various input dc current

Chapter 6

Conclusions

In this paper, we discussed noise analysis methods on translinear circuits. Because of more and more interests are focused on translinear circuit applications in recent years, actually widely being used in signal processings, the need for noise analysis arose. With the strict low-voltage, low-power demand, we need to control the noise level at output very well.

Translinear circuit shows a strongly non-linear noise behaviour, as the exponential characteristic of the transistor. Adding capacitors into the translinear circuits, the output noise becames a colored noise, see Figure 5.7. Internally, due to the existence of signal-noise intermodulation and nonstationary noise, the standard small-signal techniques are no longer applicable. Therefore, in this paper, the noise analysis methods are based on large signal equations.

Firstly, the first-order nonlinear output noise and signal-noise intermodulation of static and dynamic TL circuits are calculated on the basis of existing current-mode analysis methods. Two important noise measurements, power spectral density and signal-to-noise ratio , are specified in several generic static and dynamic TL circuit examples. This noise analysis method combines all kinds of noise sources and computes their equivalent influence at output, therefore providing PSD and SNR for the circuit designer.

Then, an alternative analysis method for DTL circuits was presented. It is a simple and direct method, because it calculates all noise sources at their original position, and does not do any moving or combining processes. In this case, it just considers the shot noise at collector terminal. Because it is the major noise source, it still provides enough accuracy for the circuit design.

Thanks to the translinear principle, we can split a big complicated circuits to many TL loops. That is to say, the above generic circuit can be applied in analyzing much more complicated circuits. In other words, we can start noise analysis at early design stage, to ensure good performance.

Reference

1. B. Gilbert, *Translinear Circuit: A Historical Overview*, Analog Integrated Circuits and Signal Processing, Vol. 9, No. 2, pp. 95 – 118, Mar. 1996.
2. B. Gilbert, *Aspects of Translinear Amplifier Design*, Part III of *Analog Circuit Design: Most RF Circuits, Sigma-Delta Converters and Translinear Circuits*, edited by W. Sansen, R. PLASSCHE, and J. HUIJSING, Kluwer Academic Publishers, 1996.
3. E. Seevink, *Analysis and Synthesis of Translinear Integrated Circuits*, in the series of Studies in Electrical and Electronic Engineering, Elsevier, 1988.
4. E. Seevink and R. Wiegerink, *Generalized Translinear Principle*, Journal of Solid-State Circuits, SC-26, No. 8, pp. 1198 – 1202, Aug. 1991.
5. R. Adams, *Filtering in the Log Domain*, in 63rd Conv. AES, May 1979.
6. E. Seevink, *Companding Current-Mode Integrator, A New Circuit Principle for Continuous-time Monolithic Filters*, Electron. Lett., Vol. 26, No. 24, pp. 2046 – 2047, Nov. 1990.
7. D. Frey, *Log-Domain Filtering: An Approach to Current-Mode Filtering*, Proc. Inst. Elect. Eng. G, Vol. 140, No. 6, pp. 406 – 416, Dec. 1993.
8. A. Woerd, J.Mulder, W. Serdijn, and A. Roermund, *Recent Trends in Translinear Circuits*, Proc. Electronic ET'96, Sozopol, Bulgaria, Vol. 1, pp. 14 – 21, 1996.
9. J. Mulder, W. Serdijn, A. Woerd, and A. Roermund, *Analysis and Synthesis of Dynamic Translinear Circuits*, Proc. ECCTD, Vol.1, pp. 18 – 23, 1997.
10. J. Mulder, A. Woerd, W. Serdijn, and A. Roermund, *General Current-Mode Analysis Method for Translinear Filters*, IEEE Trans. Circuits Syst. I, Vol. 44, pp. 193 – 197, Mar. 1997.
11. J. Mulder, *Static and Dynamic Translinear Circuits*, Neitherland: Delft University Press, 1998.
12. J. Mulder, W. Serdijn, A. Woerd, and A. Roermund, *Dynamic Translinear and Log-Domain Circuits: Analysis and Synthesis*, Kluwer Academic Publishers, 1999.
13. J. Voorman, *Continuous-time Analog Integrated Filters, in Integrated Continuous-time Filters*, Y. Tsividis and J. Voorman, Eds. IEEE Press, New York, 1993.
14. J. Mulder, A. Woerd, W. Serdijn, and A. Roermund, *An RMS-DC Converter based on the Dynamical Translinear Principle*, Proc. ESSCIRC, pp. 312 – 315, 1996.
15. Y. Tsividis, Externally-Linear, *Time-Invariant Systems and Their Application to Companding Signal Processors*, IEEE Trans. on CAS II, Vol. 44, No. 2, pp.65 – 85, Feb. 1997.
16. M. Kouwenhoven, J. Mulder, and A. Roermund, *Noise Analysis of Dynamically*

Nonlinear Translinear Circuits, Elec. Letters, Vol. 34, No. 8, pp. 705 – 706, Apr. 1998.

17. A. Ng, J. Sewell, *Direct Noise Analysis of Log-Domain Filters*, IEEE Trans. On Circuits and Systems – II, Analog and Digital Signal Processing, Vol. 49, No. 2, pp. 101 – 109, Feb 2002.
18. F. Yuan and A.Opal, *Noise and Sensitivity Analysis of Periodically Switched Linear Circuits in Frequency Domain*, IEEE Transactions On Circuits and Systems-I: Fundamental Theory and Applications, Vol. 47, No. 7, pp. 986 – 998, July 2000
19. A.Demir, J. Roychowdhury, *Modeling and Simulation of Noise in Analog/Mixed-Signal Communication Systems*, Proceedings of the IEEE Custom Integrated Circuits Conference, pp. 385 – 392, 1999.
20. P. Gary and R. Meyer, *Analysis and Design of Analog Integrated Circuits*, Third Edition, John Wiley & Sons Inc., 1993.
21. P. Gray, P. Hurst, S. Lewis, and R. Meyer, *Analysis and Design of Analog Integrated Circuits*, Fourth Edition, John Wiley & Sons Inc., 2001.
22. M. Okumura, H. Tanimoto, *T. Itakura, and T. Sugawara, Numerical Noise Analysis for Nonlinear Circuits with a Periodic Large Signal Excitation Including Cyclostationary Noise Sources*, IEEE Trans. on Circuits and Systems-I: Fundamental theory and applications, Vol.40, No.9, pp. 581 – 590, September 1993.
23. J. Mulder, M. Kouwenhoven, and A. Roermund, *Signal – Noise Intermodulation in Translinear Filters, Electronic Letters*, Vol. 33, No. 14, pp. 1205 – 1207, July 1997.
24. M. Punzenberger and C. Enz, *Noise in Instantaneous Companding Filters*, Proceedings of the IEEE International Symposium on Circuits and Systems, pp. 337 – 340, June 9-12, 1997, Hong Kong.
25. M. Punzenberger and C. Enz, *Noise in High-Order Log-Domain Filters*, Circuits and Systems, 1998. ISCAS '98. Proceedings of the 1998 IEEE International Symposium on , Vol. 1 , pp: 329 – 322, May-June 1998.
26. J. Mulder, M. Kouwenhover, W. Serdijn, A. Woerd, and A. Roermund, *Noise Considerations for Translinear Filters*, IEEE Trans. on Circuits and Systems-II: Analog and Digital Signal Processing, Vol. 45, No. 9, pp. 1199 – 1204, Sep. 1998.
27. D. Frey, *State-Space Synthesis and Analysis of Log-Domain Filters*, IEEE Trans. on Circuits and Systems-II: Analog and Digital Signal Processing, Vol. 45, No. 9, pp. 1205 – 1211, Sep. 1998.
28. L. Toth, Y. Tsividis, and N. Krishnapura, *On the Analysis of Noise and Interference in Instantaneously Companding Signal Processors*, IEEE Trans. on Circuits and Systems-II: Analog and Digital Signal Processing, Vol. 45, No. 9, pp. 1242 – 1249, Sep. 1998.
29. J. Mulder, M. Kouwenhover, W. Serdijn, A. Woerd, and A. Roermund, *Nonlinear*

Analysis of Noise in Static and Dynamic Translinear Circuits, IEEE Trans. on Circuits and Systems-II: Analog and Digital Signal Processing, Vol. 46, No. 3, pp. 266 – 278, Mar. 1999.

30. L. Toth, G. Efthivoulidis, and Y. Tsividis, *Noise Analysis of Externally Linear Systems*, IEEE Trans. on Circuits and Systems-II: Analog and Digital Signal Processing, Vol. 47, No. 12, pp. 1365 – 1377, Dec. 2000.
31. A. Ng, J. Sewell, E. Drakakis, A. Payne, and C. Toumazou, *A Unified Matrix Method for Systematic Synthesis of Log-Domain Ladder Filters*, ISCAS 2001, The 2001 IEEE International Symposium on Circuits and Systems, Vol. 1, pp. 149 – 152, May 2001.
32. D. Frey, Y. Tsividis, G. Efthivoulidis, and N. Krishnapura, *Syllabic-Companding Log Domain Filters*, IEEE Trans. on Circuits and Systems-II: Analog and Digital Signal Processing, Vol. 48, No. 4, pp. 329 – 339, Apr. 2001.
33. R. Wiegerink, *Analysis and synthesis of MOS translinear circuits*, Boston: Kluwer Academic, 1993.